Performance Analysis of an OFDM System in the Presence of Carrier Frequency Offset, Phase Noise and Timing Jitter
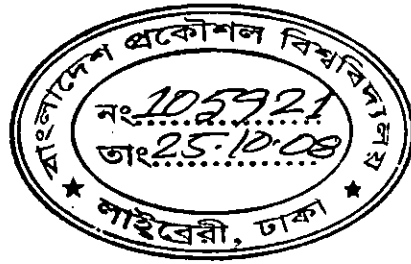
by

Shankhanaad Mallick

A thesis submitted in partial fulfillment of the requirements for the degree of

MASTER OF SCIENCE
IN
ELECTRICAL AND ELECTRONIC ENGINEERING

Department of Electrical and Electronic Engineering
BANGLADESH UNIVERSITY OF ENGINEERING AND TECHNOLOGY
September 2008

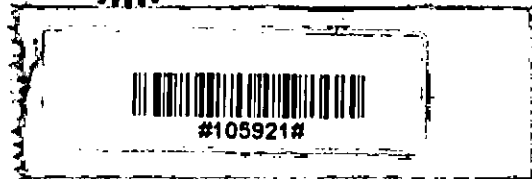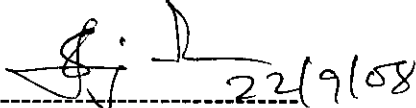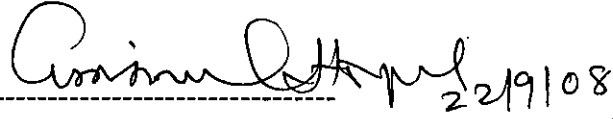The thesis titled "**PERFORMANCE ANALYSIS OF AN OFDM SYSTEM IN THE PRESENCE OF CARRIER FREQUENCY OFFSET, PHASE NOISE AND TIMING JITTER**" submitted by **SHANKHANAAD MALLICK** Roll No: 100606225 P, Session: October 2006 has been accepted as satisfactory in partial fulfillment of the requirement for the degree of **MASTER OF SCIENCE IN ELECTRICAL AND ELECTRONIC ENGINEERING** on 22nd September, 2008.
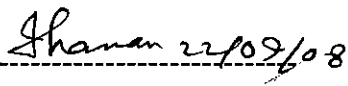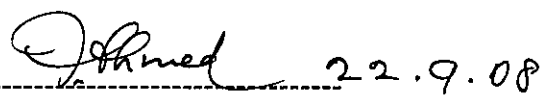
BOARD OF EXAMINERS

1. ────────────────────
   Dr. Satya Prasad Majumder   **Chairman**
   Professor
   Department of EEE, BUET
   Dhaka-1000, Bangladesh

2. ────────────────────
   Dr. Aminul Hoque   **Member**
   Professor and Head   (Ex-Officio)
   Department of EEE, BUET
   Dhaka-1000, Bangladesh

3. ────────────────────
   Dr. Imamul Hassan Bhuiyan   **Member**
   Assistant Professor
   Department of EEE, BUET
   Dhaka-1000, Bangladesh

4. ────────────────────
   Dr. Farruk Ahmed   **Member (External)**
   Professor, Department of CSE
   North South University
   (Ex Professor, Dept. of Applied Physics & Electronics
   University of Dhaka)

CANDIDATE'S DECLARATION

It is hereby declared that this thesis or any part of it has not been submitted elsewhere for the award of any degree or diploma.

Signature of the Candidate

(signature) 22/09/08

SHANKHANAAD MALLICK
Roll No: 100606225 P

ACKNOWLEDGEMENT

ABSTRACT

Multicarrier modulation exhibits significant sensitivity to the synchronization errors. A theoretical analysis for evaluating the performance of an Orthogonal Frequency Division Multiplexing (OFDM) under the combined influence of Carrier Frequency Offset (CFO), phase noise and timing jitter over Rayleigh fading channels is presented in this dissertation. An exact closed form expression for the Signal-to-Interference-plus-Noise Ratio (SINR) is derived and the combined effects of these synchronization impairments are exhibited by expressing the OFDM system bit error rate (BER) performance as a function of its critical parameters. It is shown by analysis that OFDM system suffers significant SINR penalty due to CFO and jitter, however, the effect of phase noise is the dominant one. The performance degradation also depends on the system parameters, such as number of subcarriers, phase noise linewidth, transmission data rate, modulation level and SNR. In this scenario, the BER performance improvements through turbo coding and diversity techniques are evaluated and parameter selection criteria for turbo coded OFDM operated at different SNR level are analyzed.

TABLE OF CONTENTS

Chapter 1

INTRODUCTION

Chapter 2

CONCEPT OF WIRELESS CHANNEL & OFDM

Chapter 3

INFLUENCE OF CARRIER FREQUENCY OFFSET (CFO), PHASE NOISE AND TIMING JITTER ON UNCODED OFDM SYSTEMS

Chapter 4

PERFORMANCE IMPROVEMENT TECHNIQUES: TURBO CODING & DIVERSITY

Chapter 5

RESULTS AND DISCUSSION

Chapter 6

CONCLUSIONS AND FUTURE WORK

LIST OF TABLES

ix

LIST OF FIGURES

LIST OF IMPORTANT ABBREVIATIONS

ADSL	Asymmetric Digital Subscriber Line
AWGN	Additive White Gaussian Noise
BER	Bit Error Rate
BPSK	Binary Phase Shift Keying
CFO	Carrier Frequency Offset
COFDM	Coded Orthogonal Frequency Division Multiplexing
CP	Cyclic Prefix
CSI	Channel State Information
DAB	Digital Audio Broadcasting
DFT	Discrete Fourier Transform
DPSK	Differential Phase Shift Keying
DVB	Digital Video Broadcasting
FDM	Frequency-Division Multiplexing
FDMA	Frequency Division Multiple Access
FFT	Fast Fourier Transform
GI	Guard Interval
GSM	General System for Mobile Communication.
ICI	Inter-Carrier Interference
IDFT	Inverse Discrete Fourier Transform
IFFT	Inverse Fast Fourier Transform
ISI	Inter-Symbol Interference
ITU	International Telecommunication Union
LOS	Line of Sight
MAC	Media Access Control
MC-CDMA	Multi-carrier Code Division Multiple Access
MCM	Multi-Carrier Modulation
MIMO	Multiple-Input Multiple-Output
MISO	Multiple Input Single Output
MRC	Maximal-Ratio Combining

OFDM	Orthogonal Frequency Division Multiplexing.
OFDMA	Orthogonal Frequency Division Multiple Access
PAPR	Peak-to-Average Power Ratio
QAM	Quadrature Amplitude Modulation
QPSK	Quadrature Phase Shift Keying
SER	Symbol Error Rate
SIMO	Single Input Multiple Output
SISO	Single Input Single Output
SNR	Signal to Noise Ratio
SINR	Signal to Interference plus Noise Ratio
STBC	Space-Time Block Code
TDM	Time-Division Multiplexing
TDMA	Time Division Multiple Access.
UMTS	Universal Mobile Telecommunications System.
WLAN	Wireless Local Area Network

CHAPTER 1

INTRODUCTION
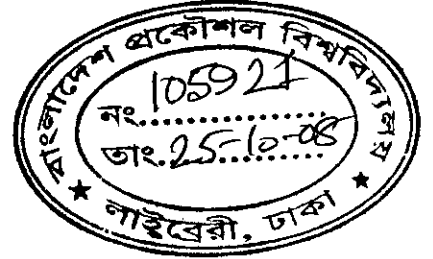
1.1 Motivation for the Research

Wireless Communication with mobile phones and Wireless Local Area Networks (WLANs) has become a part of human life. Equipped with a wireless card, a laptop allows people to work at any place in the office. More and more wireless multimedia services are expected in the future. This creates an ever-increasing demand for bandwidth. On the other hand, frequency is a finite resource. Thus, bandwidth efficient transmission techniques are urgently required.

The unpredictable nature for example, multipath fading, Doppler spread, and time dispersion of wireless channel is a major limiting factor for a high data rate and high quality wireless communication system. Due to multipath fading, different echoes of transmitted symbols overlap at the receiving end, which may lead to inter-symbol interference (ISI). In a multipath channel, most conventional modulation techniques are sensitive to ISI unless the symbol period is much larger compared to the delay spread of the channel. One way to effectively combat the channel impairments and still provide high-data rates in a limited bandwidth is use of Multicarrier Modulation (MCM) method.

Orthogonal Frequency Division Multiplexing (OFDM) is a multi-carrier modulation technique that allows bandwidth efficient data transmission with a low complexity transceiver. Being very efficient in combating multipath fading as well as Inter Symbol Interference (ISI), OFDM has been widely adopted and implemented in wire and wireless communications, such as Digital Subscriber Line (DSL), European Digital Audio Broadcasting (DAB), Digital Video Broadcasting-Terrestrial (DVB-T) and its handheld version DVB-H, and IEEE 802.11a/g standards for WLANs [1]-[2].

Unfortunately OFDM, like other Multi-Carrier Modulation (MCM) systems, is very much sensitive to the synchronization errors such as carrier frequency offset (CFO), timing jitter and phase noise [3]. The CFO arises mainly due to the Doppler shifts introduced by the channel which causes frequency difference between the transmitter and receiver oscillators. The effects caused by the CFO are the reduction of the signal amplitude and introduction of Inter-Carrier-Interference (ICI) from the other carriers which are now no longer orthogonal to the filter [4]. Phase noise is a random process results from the imperfections of the Local Oscillators (LO) used for the conversion of the baseband signal to a passband (or vice-versa). Phase noise causes leakage of DFT, which subsequently destroys the orthogonalities among subcarrier signals. Phase noise has two effects on an OFDM system: rotation of the symbols over all subcarriers by a Common Phase Error (CPE) and the occurrence of ICI which introduces a blurring of the constellation like thermal noise [5]. Timing errors would occur either when the clock signal is not correctly recovered, or when sampling is not performed at precise sampling instants. Because of the non-ideal nature of the sampling circuit, the amplitude of the signal is affected by timing jitter and also introduces additive noise [6].

The individual effects of CFO and phase noise have been analyzed by several authors and the degradation introduced in the system has been characterized for some particular cases in [3]-[5], [7]-[12]. The effect of timing jitter on the performance of discrete multitone system was also investigated in [13] and in [14]. However, a closed form analytical result that shows the exact quantitative effect of the combination of these three impairments even for Additive White Gaussian Noise (AWGN) channels has not been well addressed.

1.2 Objectives of this Thesis Work

The objectives and possible outcomes of this thesis work are:

- To develop an analytical model for an OFDM system taking into considerations the combined influence of CFO, phase noise and timing jitter over Rayleigh fading channel.

- Derivation of the exact SINR expression in a closed form as a function of these synchronization errors.

- Bit Error Rate (BER) performance evaluation of a BPSK-OFDM system under the influence of these synchronization impairments over Rayleigh fading channel and comparison of the system performance by changing its modulation level (M-ary PSK).

- To evaluate the SINR penalty suffered by the system for different combination of variances of CFO, phase noise and timing jitter for a given channel SNR.

- BER performance analysis of Coded-OFDM (COFDM) systems with synchronization impairments by applying turbo coding and evaluation of the performance improvement.

- To analyze the parameter selection criteria for a turbo-coded OFDM operated at different SNR level.

- BER performance evaluation of a BPSK-OFDM in the presence of CFO, phase noise and timing jitter with antenna diversity using maximal ratio combining method.

1.3 Organization of the Research

The outline of this thesis is organized as follows. Chapter 2 describes the basic concepts required for a better understanding of this work. A description of the wireless radio channel is given first. Then, traditional multiplexing and the corresponding multiple access methods are introduced. The need for a Multi-Carrier Modulation (MCM) and OFDM are explained afterwards. Then a detailed discussion on the principle, parameters, properties and drawbacks of OFDM system is given. The chapter ends with a brief discussion of the synchronization errors encountered in OFDM systems.

A theoretical analysis for evaluating the performance of the uncoded OFDM systems under the combined influence of Carrier frequency offset (CFO), phase noise and timing jitter is presented in Chapter 3.

Chapter 4 is based on the performance improvement techniques for uncoded OFDM with synchronization errors. At first, the need for coding and diversity for uncoded OFDM is explained and a brief overview of turbo coding is given afterwards. Then the factors that affect the BER performance of turbo codes are analyzed and the design criteria for turbo codes at different SNR level are discussed. The BER expression for turbo coded OFDM with synchronization impairments are evaluated to examine the performance improvement. At the end of the chapter the performance improvements through diversity combining methods are evaluated.

In Chapter 5, the performance results for the uncoded OFDM system model developed in Chapter 3 are illustrated and analyzed. Then the performance improvement results through turbo coding and antenna diversity are discussed. Finally the thesis ends with a summary and suggestions for future research.

CHAPTER 2

CONCEPT OF WIRELESS CHANNEL & OFDM

2.1   Introduction

This chapter introduces some basic concepts used in the following chapters which are required for the understanding of this work. We begin with a review of the wireless radio channels in Section 2.2. The importance of multiple access for communication systems is then explained in Section 2.3 together with the classification of different multiplexing and multiple access methods. The need for multicarrier modulation (MCM) in wireless systems is explained briefly in Section 2.4. Orthogonal Frequency Division Multiplexing (OFDM) is first introduced in Section 2.5 as an efficient realization of MCM technique. The basic principle, parameters, properties and drawbacks of OFDM are described. Finally Section 2.6 gives an overview of the synchronization errors encountered in OFDM. The impacts of Carrier Frequency Offset (CFO), phase noise and timing jitter on OFDM transmission are discussed briefly.

2.2   The Wireless Radio Channel

The wireless radio channel is defined as the space between the antennas of the transmitter and the receiver. The special conditions under which the radio wave propagation takes place have significant impact on the performance of communication systems [15]. This section is intended to review the features of wireless radio channels, their mathematical description, and statistical properties.

2.2.1   Two important features

Two important features of the wireless radio channels have significant influence on the signal arriving at the receiver antenna: multipath propagation and time variance.

Multipath propagation:

In a typical wireless propagation channel, due to the existence of obstacles, the electromagnetic waves from the transmitter antenna can experience reflection, scattering or diffraction before reaching receive antennas. In other words, the transmitted wave can arrive at the receiver through several different paths with possibly different propagation delay (Fig. 2.1).
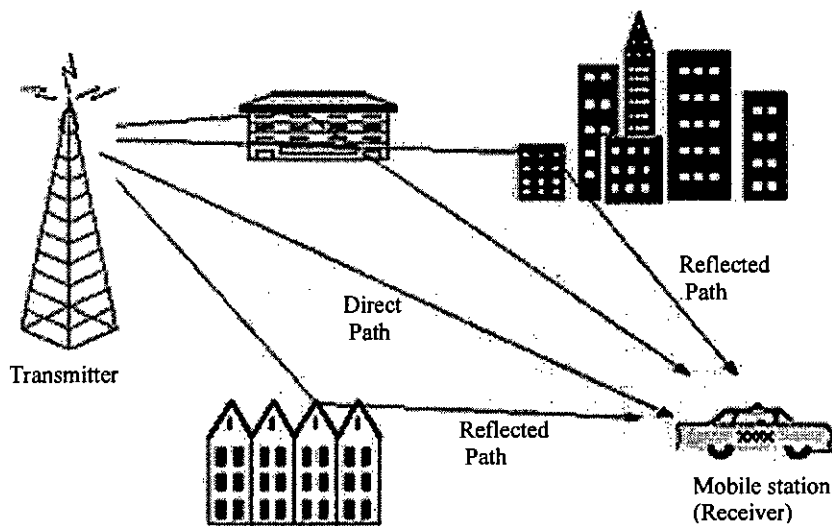
Fig. 2.1: Multipath propagation

Such phenomenon is called multipath propagation, which introduces the time spread into the signal that is transmitted through the channel. For this reason, at the receiver the received signal is the superposition of several replicas of the transmitted signal. Each replica has its specific amplitude weighting, time delay and phase shift. These replicas can add constructively or destructively, dependent on their relative phase. As a result, the total power of the resulting received signals varies with the relative phase, which is a function of carrier frequency and the relative propagation delay. This variation in the receiver power is called signal fading. If the bandwidth of the transmitted signal is much smaller than the coherence bandwidth of the channel, the channel is thus called flat fading channel. In contrast to flat fading, frequency selective fading is caused if the band-width of the

transmitted signal is much larger than the coherence bandwidth of the channel. In consequence, different spectral components of the signal have different gains (frequency transfer functions), and inter-symbol interference (ISI) is introduced.

Time variance:

Time variance is an inherent feature of most wireless channels. It results not only from the position change of the transmitter and receiver, or an obstacle changing its position, but also from the time variation of the medium. In one word, the channel varies with time because of mobility. Accordingly, the amplitude as well as the phase of the received signals will also change with time. Mobility also leads to a shift of the received frequency, called Doppler shift (f_d). For instance, in a narrowband mobile channel, Doppler shift is a function of the carrier frequency f_c and the movement speed in the direction of wave propagation, given by

$$f_d = f_c \cdot \frac{v}{c} \cos \zeta \qquad (2.1)$$

where v is the velocity of movement, c is the velocity of light, and ζ represents the azimuthal angle between direction of wave and direction of relative receiver movement. The received frequency is therefore described as

$$f = f_c - f_d \qquad (2.2)$$

and distributed in the range [$f_c - f_{d\max}$, $f_c + f_{d\max}$], where $f_{d\max} = +f_c \cdot \frac{v_{\max}}{c}$ If there exist multiple paths, we need to know the power distribution of incident waves, i.e., the Doppler power spectral density, $S_D(f_d)$, which can be plotted as a function of f_d ,

$$S_D(f_d) = \begin{cases} \dfrac{con\,st\,ant}{\pi \sqrt{f_{d\max}^2 - f_d^2}} & for\ |f_d| \le f_{d\max}, \\ 0 & otherwise \end{cases} \qquad (2.3)$$

An example of Doppler spectrum is plotted in Fig 2.2.
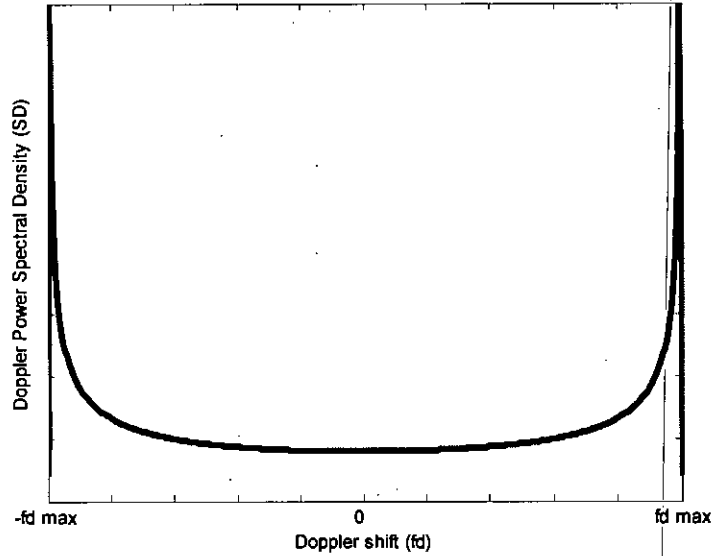
Fig. 2.2: Jakes Doppler Power Spectrum

Furthermore, if the channel impulse response (CIR) varies significantly in a symbol duration, or equivalently, in the frequency domain the Doppler spread B_D ($B_D = f_{d\,max}$) is larger than the signal bandwidth, then the signal undergoes fast fading; By contrast, if B_D is much smaller than the signal bandwidth, the signal undergoes slow fading; In addition, the channel is considered time-invariant if the transmitter , the receiver, and the medium between them are static. Most wireless channels can be classified as slowly time-variant systems, also known as quasi-static.

In general, the time variations of the channel appear to be unpredictable to the user. Therefore, it is reasonable to characterize the time-variant multipath channel statistically [16]. In the following we give a tapped delay line model for the mathematical description of the channel.

2.2.2 Mathematical description of the channel

Tapped delay line model:

By means of the time-variant channel impulse response, we can give a simple but comprehensive mathematical description of a time-variant multipath channel. The equivalent low-pass channel model is described as [17]

$$h(t,\tau) = \sum_{l=0}^{L-1} c_l(t)\,\delta(\tau - \tau_l(t)) = \sum_{l=0}^{L-1} |c_l(t)| e^{j\theta_l(t,\tau)} \delta(\tau - \tau_l(t)) \tag{2.4}$$

The parameters in (2.4) are described as follows:

- $\tau_l(t)$ = time-variant propagation delay where $\tau_0(t)$ is assumed to be zero;

- $c_l(t)$ = time-variant equivalent low-pass tap weighting;

- $|c_l(t)|$ = amplitude of $c_l(t)$;

- $\theta_l(t)$ = time variance phase of $c_l(t)$.
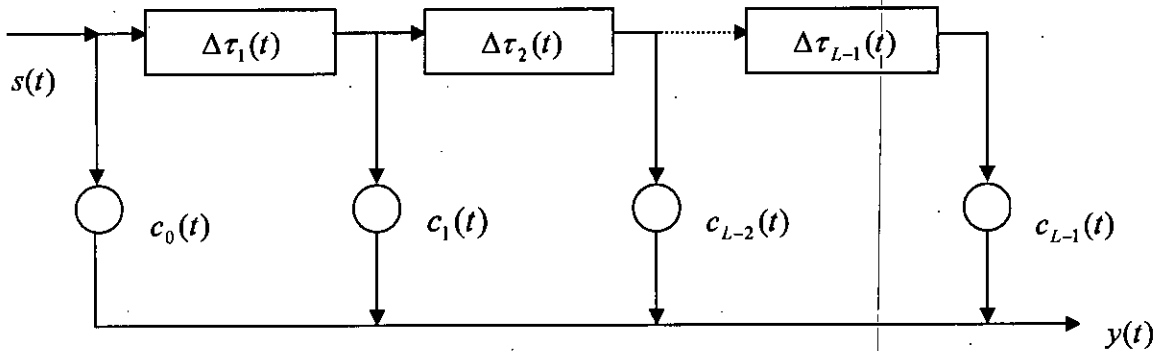
Fig. 2.3: Tapped delay line model of the wireless channel

Fig. 2.3 illustrates such a channel model, where $\Delta\tau_l(t)$ represents the delay difference between $\tau_l(t)$ and $\tau_{l-1}(t)$. It is reasonable to suppose hat signals via several different paths arrive at the receiver at the same time, i.e. have the same propagation delay. Equation (2.4) is therefore rewritten as

$$h(t,\tau) = \sum_{l=0}^{L-1} \sum_{k} a_{l,k}(t)\delta(\tau - \tau_l(t)) = \sum_{l=0}^{L-1} \sum_{k} |a_{l,k}(t)| e^{j\varphi_{l,k}(t)} \delta(\tau - \tau_l(t)) \qquad (2.5)$$

Furthermore, if the autocorrelation functions of stochastic process $a_{l,k}(t)$ are independent of the absolute time t, and different weights $a_{l,k}(t)$ are mutually correlated, i.e., the complex-valued tap weighting $a_{l,k}(t)$ is wide sense stationary (WSS), and uncorrelated scattering (US), channel model in (2.5) is called a WSSUS model.

If there exists no direct path between the transmitter and the receiver, we have a non-line-of-sight (NLOS) channel. In such a case any individual multipath component $a_{l,k}(t)$ can be modeled as a complex-valued Gaussian process, and in consequence the envelopes $|a_{l,k}(t)|$ at any instant t are Rayleigh distributed [18]. A Rayleigh distribution has a probability density function (PDF)

$$p(r) = \begin{cases} \dfrac{r}{\sigma^2} e^{-[\frac{r^2}{2\sigma^2}]} & \text{for } r \geq 0; \\ 0 & \text{otherwise} \end{cases} \qquad (2.6)$$

The phase of $a_{l,k}(t)$ is uniformly distributed in the range of $(0, 2\pi)$. Moreover, $c_l(t)$ as well as $h(t,\tau)$ have the same statistical properties as $a_{l,k}(t)$. On the other hand, it there exists a line-of-sight (LOS) path, i.e., a dominant stationary non-faded path component, the envelope of $h(t,\tau)$ has Rician distribution. More details about the wireless channel can be seen in [15], [16], [17], [18] and [19].

2.3   Multiplexing and Multiple Access

Multiplexing and multiple access refer to the sharing of a common transmission channel by a number of different users. In general, multiplexing is the transmission of information from several sources, located at the same site, to several destinations over the same transmission channel. We emphasize 'sources' instead of 'users', since they are likely to

belong to a single user. Multiple access, however, aims for containing multiple users in a communication system, where different users are located over a large geographical region, and share a common destination, like a base station (in a cellular radio network). For a given channel, the multiplexing can be done by subdividing the channel capacity in to a number of portions (channel division multiplexing) and assigning a portion to each traffic source. The channel division multiplexing can be done in different ways. Furthermore, each multiple access method has a corresponding multiplexing method, i.e.,

multiplexing method$\longleftrightarrow$ multiple access method

(a) FDM (b) TDM (c) CDM
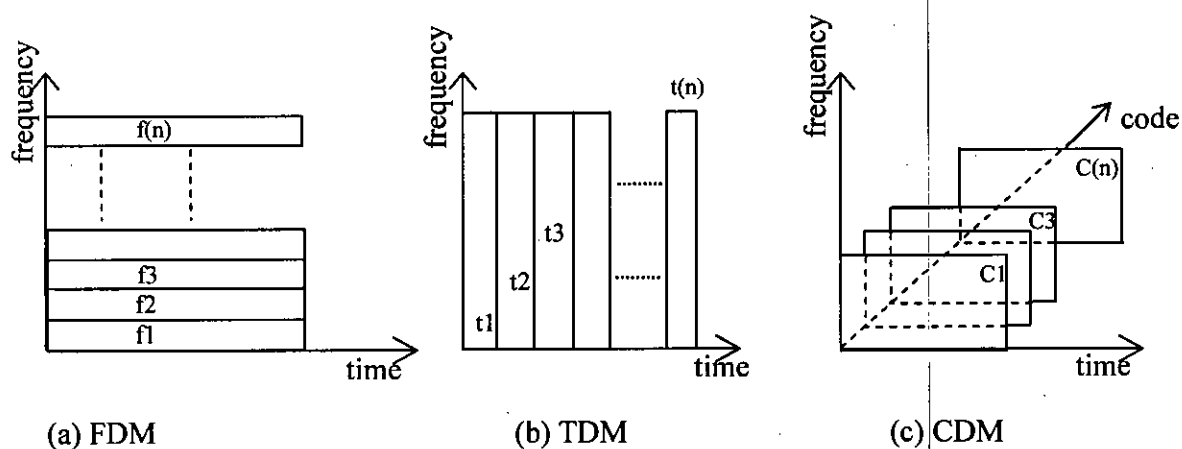
Figure 2.4: Multiplexing techniques

FDM/FDMA: One simple way to multiplex a channel is frequency division multiplexing (FDM) where the available channel bandwidth is subdivided into many no-overlapping sub-bands, which are so-called frequency division channels, as illustrated in Fig. 2.4(a). With FDM, signals in different sub-bands can be transmitted simultaneously over the same physical medium. Accordingly, in a frequency division multiple access (FDMA) system, each user accessing the base station is allocated a unique channel or sub-band. FDMA system us usually a narrowband system since the bandwidth of FDMA channels is relatively narrow. In addition, FDMA is not bandwidth efficient in that the channels are

non-overlapping and once a channel is set to a specific user, it can not be used by other users even if it is not in use and stays idle.

TDM/TDMA   With time division multiplexing (TDM) the radio spectrum is divided into time slots. Each time slot is a so-called time division channel, and each signal is transmitted one at a time in different time slots using the full frequency bandwidth, as shown in Fig. 2.4(b). In a time division multiple access (TDMA) system, an individual user is assigned one or several time slots on demand. Moreover, data transmission for users in such a system is not continuous but occurs in bursts. Such burst transmission results in larger overhead in TDMA for the synchronization as well as larger guard time as compared to FDMA.

CDM/CDMA   By multiplying with a wideband signal, a narrowband signal is converted into a wideband noise-like signal before transmission. Such wideband signal is so-called spreading signal, which is a code sequence having a chip rate that is orders of the rate of the message. Simultaneously, transmitted narrowband signals are assigned by specific code sequences so that Code division multiplexing (CDM) is realized, see Fig. 2.4(c). Code sequences are carefully selected to ensure that each of them is orthogonal to or approximately orthogonal to others. A code division multiple access (CDMA) is inherently a wideband transmission system, where signals of different users overlap in both time and frequency, and are separated by using orthogonally coded spread spectrum modulation.

2.4   Need for Multicarrier Modulation (MCM)

Now-a-days wireless communication systems require high data rate multimedia services such as audio, data, image and video. In order to provide these services, a high data rate and high quality digital communication system is required in a restricted bandwidth. A major limiting factor is the unpredictable wireless channel condition because of the factors such as multipath fading, Doppler spread, and time dispersion or delay spread. It causes frequency-selective fading due to different echoes of transmitted symbols overlapping at the receiving end, which can lead to the bit-error-rate (BER) degradation. In a multipath channel, most conventional modulation techniques are sensitive to inter-symbol

interference (ISI) unless the channel symbol rate is small compared to the delay spread of the channel. One way to effectively combat the channel impairments and still provide high-data rates in a limited bandwidth is use of Multicarrier Modulation (MCM) method.

Orthogonal Frequency Division Multiplexing (OFDM) is an attractive multicarrier modulation (MCM) technique because of its high spectral efficiency with a low complexity transceiver [19]. OFDM was first proposed by Chang in 1966 [20]. It is different from FDM in several ways. Typically with FDM the transmission signals need to have a large frequency guard-band between channels to prevent interference. This lowers the overall spectral efficiency. However, with OFDM the orthogonal packing of the subcarriers greatly reduces this guard band, improving the spectral efficiency.

In an OFDM scheme, a large number of orthogonal, overlapping, narrow band sub-channels or subcarriers, transmitted in parallel, divide the available transmission bandwidth. The separation of the subcarriers is theoretically minimal such that there is a very compact spectral utilization. The attraction of OFDM is mainly due to how the system handles the multipath interference at the receiver. Multipath generates two effects: frequency selective fading and inter-symbol interference (ISI). The "flatness" perceived by a narrow-band channel overcomes the former, and modulating at a very low symbol rate, which makes the symbols much longer than the channel impulse response, diminishes the latter. Using powerful error correcting codes together with time and frequency interleaving yields even more robustness against frequency selective fading and the insertion of an extra guard interval between consecutive OFDM symbols can reduce the effects of ISI even more. Thus, an equalizer in the receiver is not necessary.

OFDM has been widely adopted and implemented in wire and wireless communications, such as Digital Subscriber Line (DSL), European Digital Audio Broadcasting (DAB), Digital Video Broadcasting-Terrestrial (DVB-T) and its handheld version DVB-H, and IEEE 802.11a/g standards for WLANs.

A detailed description of OFDM is provided in the following section.

2.5   Basic Principles of OFDM

2.5.1   Orthogonality

Signals are orthogonal if they are mutually independent of each other. Orthogonality is a property that allows multiple information signals to be transmitted perfectly over a common channel and detected without interference. Loss of orthogonality results in blurring between these information signals and degradation in communications.

OFDM signals are made up from a sum of sinusoids, with each corresponding to a subcarrier. The subcarriers in an OFDM signal are spaced as close as is theoretically possible while maintain orthogonality between them. The baseband frequency of each subcarrier is chosen to be an integer multiple of the inverse of the symbol time, resulting in all subcarriers having an integer number of cycles per symbol. As a consequence the subcarriers are orthogonal to each other. Fig. 2.5 shows three subcarriers, which are orthogonal to each other.

Sets of functions are orthogonal to each other if they match the conditions in equation (2.7). If any two different functions within the set are multiplied, and integrated over a symbol period, the result is zero, for orthogonal functions. Another way of thinking of this is that if we look at a matched receiver for one of the orthogonal functions, a subcarrier in the case of OFDM, then the receiver will only see the result for that function. The results from all other functions in the set integrate to zero, and thus have no effect.

$$\int_0^T s_i(t)s_f(t)dt = \begin{cases} C & i = j \\ 0 & i \neq j \end{cases} \qquad (2.7)$$
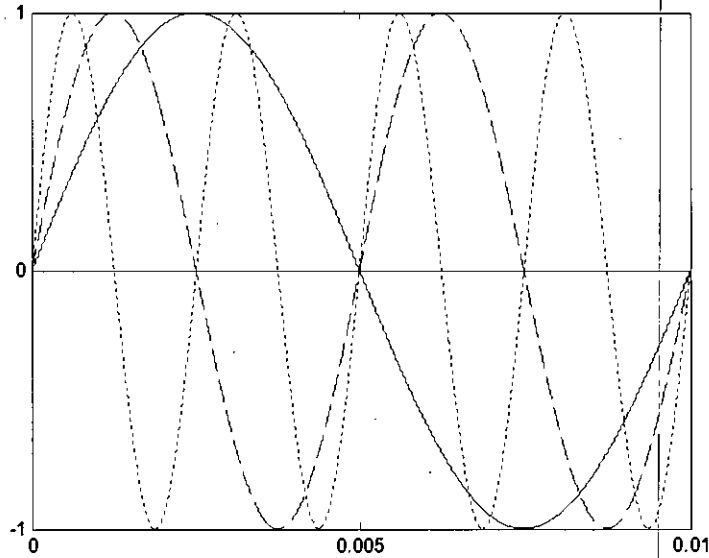
Fig. 2.5: Construction of orthogonal signals

Equation (2.8) shows a set of orthogonal sinusoids, which represent the subcarriers for an unmodulated real OFDM signal.

$$s_k(t) = \begin{cases} \sin(2\pi k f_0 t) & 0 < t < T \quad k = 1,2,...M \\ 0 & otherwise \end{cases} \tag{2.8}$$

where f_0 is the carrier spacing, M is the number of carriers, T is the symbol period. Since the highest frequency component is Mf_0, the transmission bandwidth is also Mf_0. These subcarriers are orthogonal to each other because when we multiply the waveforms of any two subcarriers and integrate over the symbol period, the result is zero.

2.5.2   Frequency domain orthogonality

Another way to view the orthogonality property of OFDM signals is to look at its spectrum. In the frequency domain, each OFDM subcarrier has a *sinc* or *sin(x)/x*, frequency response as a result of windowing in the time domain as shown in Fig. 2.6(a). The *sinc* shape has a narrow main lobe, with many side-lobes that decay slowly with the magnitude of the

frequency difference away from the centre. Each carrier has a peak at its centre frequency and nulls evenly spaced with a frequency gap equal to the carrier spacing as shown in Fig. 2.6 (b).
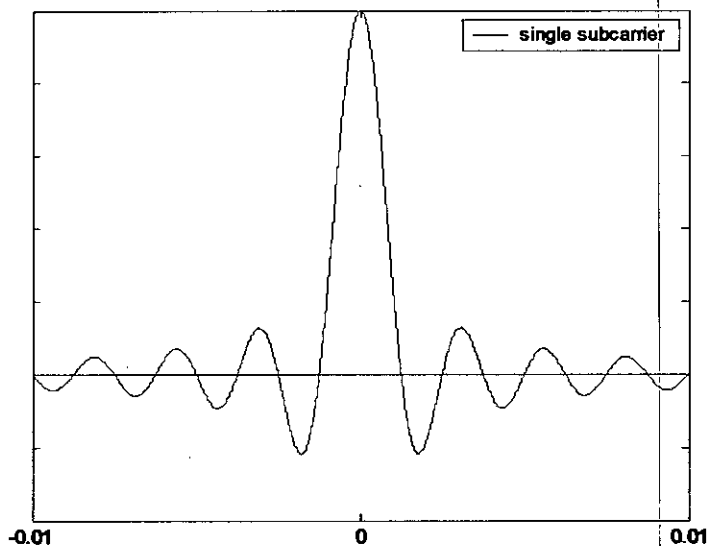
Fig. 2.6 (a): Frequency response of a single subcarrier
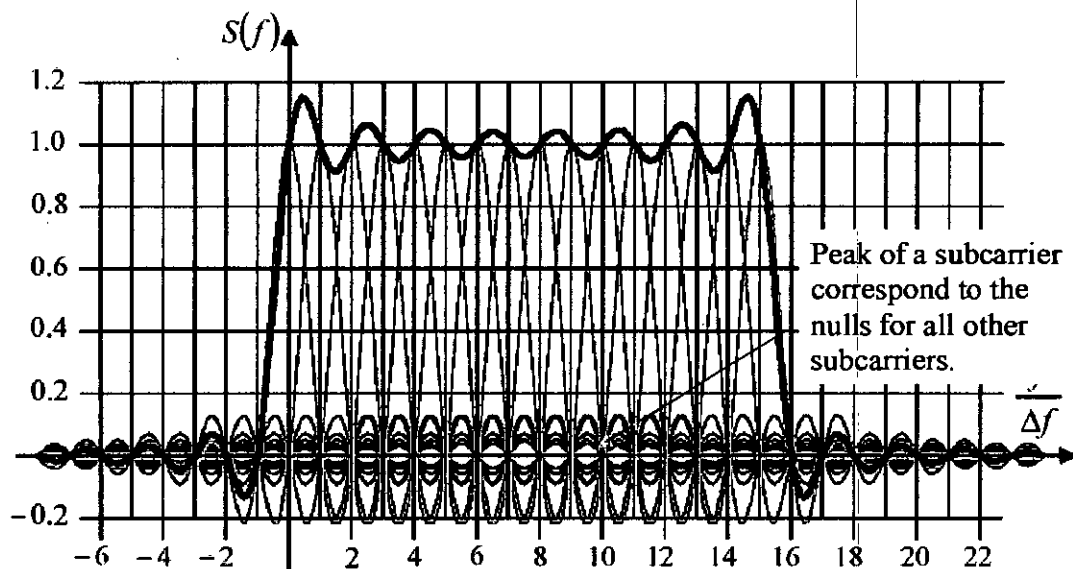
Fig. 2.6 (b): An example of OFDM spectrum with 16 subcarriers

The orthogonal nature of the transmission is a result of the peak of each subcarrier corresponding to the nulls of all other subcarriers. When this signal is detected using a Discrete Fourier Transform (DFT), the spectrum is not continuous, but has discrete samples. If the DFT is time synchronized, the frequency samples of the DFT correspond to just the peaks of the subcarriers, thus the overlapping frequency region between subcarriers does not affect the receiver. The measured peaks correspond to the nulls for all other subcarriers, resulting in orthogonality between the subcarriers.

2.5.3 OFDM generation and reception

OFDM signals are typically generated digitally by discrete Fourier transform (DFT) technique [21] due to the difficulty in creating large banks of phase lock oscillators and receivers in the analog domain. Fig. 2.7 shows the block diagram of a typical OFDM transceiver. The transmitter section converts digital data to be transmitted, into a mapping of subcarrier amplitude and phase. It then transforms this spectral representation of the data into the time domain using an Inverse Discrete Fourier Transform (IDFT) operation. The Inverse Fast Fourier Transform (IFFT) performs the same operations as an IDFT, except that it is much more computationally efficiency, and so is used in all practical systems. In order to transmit the OFDM signal the calculated time domain baseband signal is then converted to the required passband frequency by Local Oscillators (LO).

The receiver performs the reverse operation of the transmitter; down converting the RF signal to base band for processing, then using a Fast Fourier Transform (FFT) to analyze the signal in the frequency domain. The amplitude and phase of the subcarriers is then picked out and converted back to digital data.

The IFFT and the FFT are complementary function and the most appropriate term depends on whether the signal is being received or generated. In cases where the signal is independent of this distinction then the term FFT and IFFT is used interchangeably.
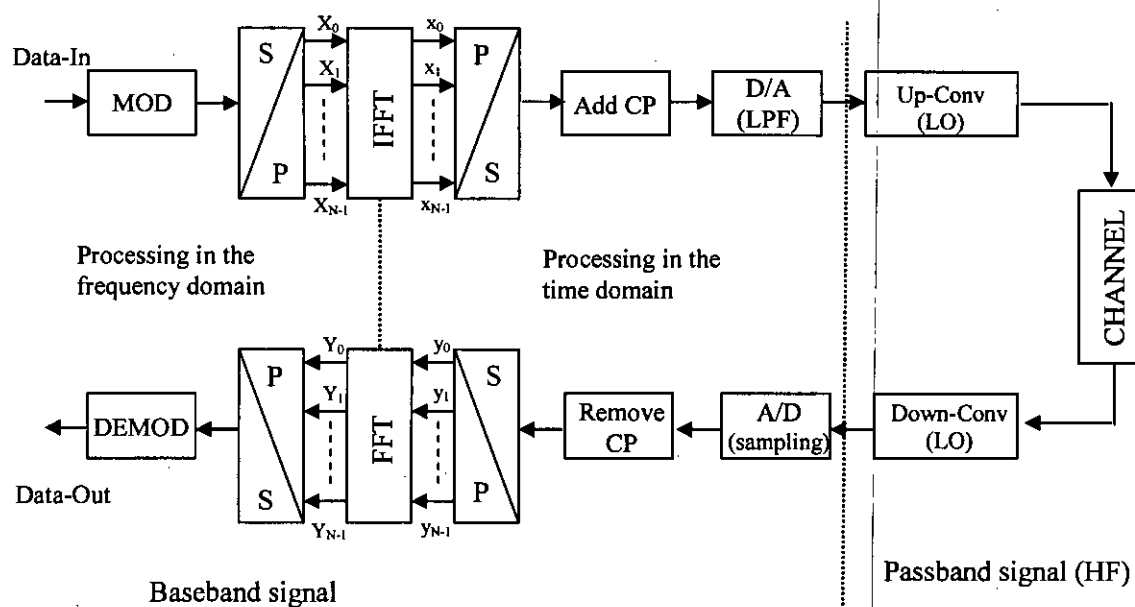
Fig. 2.7: Block diagram of a basic OFDM Transceiver

2.5.3.1 Subcarrier modulation & mapping

The serial data stream is first mapped to amplitude and phase, which is represented by a complex In-phase and Quadrature-phase (IQ) vector using a modulation scheme. Fig. 2.8(a) shows an example of subcarrier modulation & mapping. This example shows QPSK, which maps 2 bits for each symbol. Each combination of the 2 bits of data corresponds to a unique IQ vector, shown as a dot on the figure. A large number of modulation schemes are available allowing the number of bits transmitted per carrier per symbol to be varied.

In the receiver, mapping the received IQ vector back to the data word performs subcarrier demodulation. However noise corrupts the symbol constellation during transmission. Fig. 2.8 (b) shows an example of a received QPSK signal at the SNR of 10 dB.
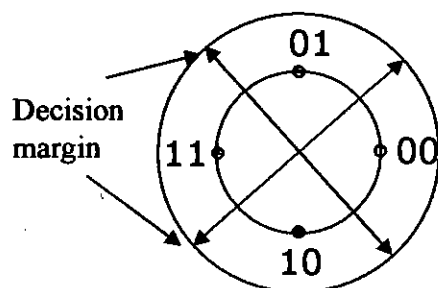
Fig. 2.8(a): IQ modulation constellation for QPSK with gray coding
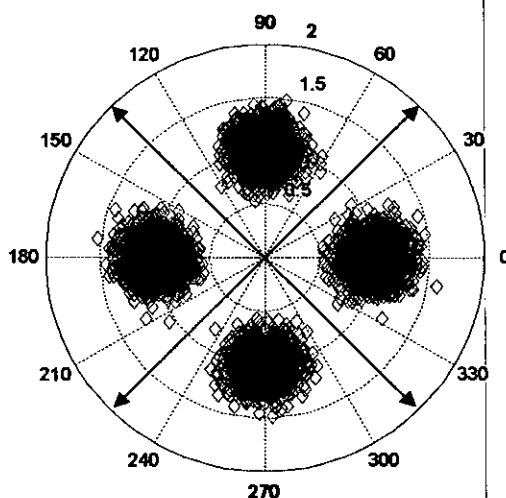
Fig. 2.8(b): IQ plot for QPSK at 10 dB SNR

Each of the IQ points is blurred in location due to the channel noise. For each received IQ vector the receiver has to estimate the most likely original transmission vector. This is achieved by finding the transmission vector that is closest to the received vector. Errors occur when the noise exceeds half the spacing between the transmission IQ points, making it cross over a decision boundary.

2.5.3.2 Serial to parallel conversion

In every OFDM symbol, each subcarrier is assigned with a modulated IQ vector by serial to parallel conversion of the modulated serial data stream. The data allocated to each OFDM symbol depends on the modulation scheme used and the number of subcarriers. For

a QPSK modulation scheme, each subcarrier is assigned to 2 bits of data and so for a transmission using 100 subcarriers, the number of bits per OFDM symbol would be 200. For adaptive modulation schemes, the modulation scheme which is used on each subcarrier can vary and so the number of bits per subcarrier also varies. At the receiver the reverse process takes place, with the data from the subcarriers being converted back to the original serial data stream. When an OFDM transmission occurs in a multipath radio environment, frequency selective fading can result in groups of subcarriers being heavily attenuated, which in turn can result in bit errors. These nulls in the frequency response of the channel can cause the information sent in neighboring carriers to be destroyed, resulting in a clustering of the bit errors in each symbol. Most Forward Error Correction (FEC) schemes tend to work more effectively if the errors are spread evenly, rather than in large clusters, and so to improve the performance most systems employ data scrambling as part of the serial to parallel conversion stage. This is implemented by randomizing the subcarrier allocation of each sequential IQ vector. At the receiver the reverse scrambling is used to decode the signal. This restores the original sequencing of the data bits, but spreads clusters of bit errors so that they are approximately uniformly distributed in time. This randomization of the location of the bit errors improves the performance of the FEC and the system as a whole.

2.5.3.3 Frequency to time domain conversion

After serial to parallel conversion, modulated data is assigned to each of the data subcarriers based on the data rate and the modulation scheme; all unused subcarriers are set to zero. This sets up the OFDM signal in the frequency domain. An IFFT is then used to convert this signal to the time domain, allowing it to be transmitted. Fig. 2.9 shows the IFFT section of the OFDM transmitter. In the frequency domain, before applying the IFFT, each of the discrete samples of the IFFT corresponds to an individual subcarrier. Most of the subcarriers are modulated with data. The outer subcarriers are unmodulated and set to zero amplitude. These zero subcarriers provide a frequency guard band before the Nyquist frequency and effectively act as an interpolation of the signal and allows for a realistic roll off in the analog anti-aliasing reconstruction filters.
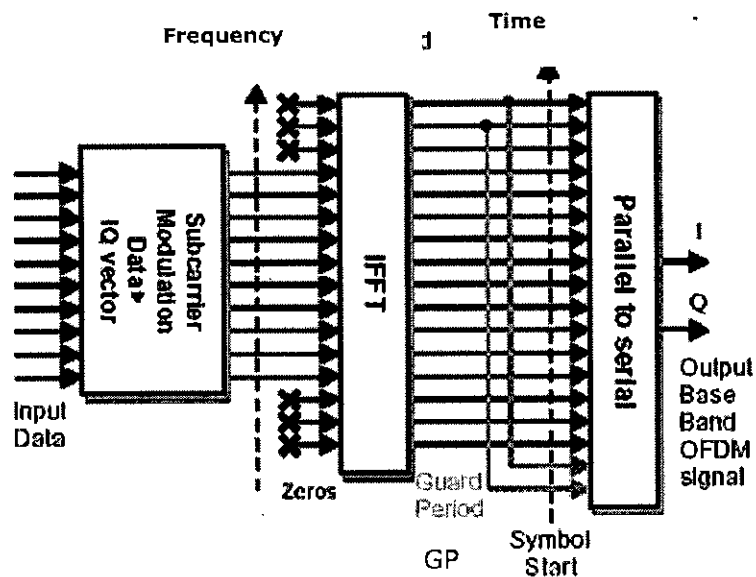
Fig. 2.9: Frequency to time domain conversion stage

2.5.3.4 Guard period insertion

A time dispersive channel, however, may corrupt the orthogonality between the subcarriers. To be specific, in the time domain ISI is introduced between OFDM symbols, and in consequence inter-carrier interference (ICI) destroys the orthogonality between the subcarriers in frequency domain. The trick to eliminate ISI in the case of a linearly distorting channel is the introduction of a guard period of a duration not less than the maximum delay spread of the channel. What's more, to maintain orthogonality, a cyclic prefix (CP) instead of an empty interval is used, which is able to remove ISI as well as ICI at the cost of extra transmit power. That is, we copy the last T_G samples of an OFDM symbol and put them at the beginning of the symbol as a prefix. (Fig. 2.10). As a consequence, the linear convolution is converted to circular convolution. The later one ensures the orthogonality between subcarriers.

At the receiver, this prefix will be discarded. If the maximum delay spread of the channel is not greater than T_G, the echoes of the last part of the previous symbol will fall into the duration of the prefix and be removed together with prefix. This is illustrated in Fig. 2.11. The remaining samples (T_{FFT}) are used for Fourier transformation (FFT).
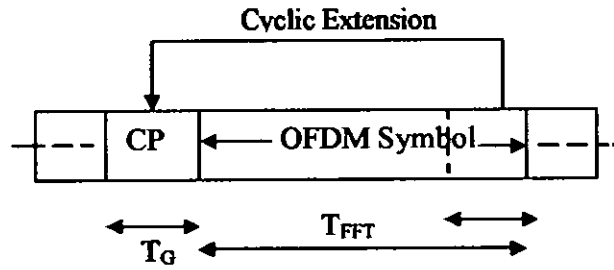
Fig. 2.10: Addition of a guard period to an OFDM signal
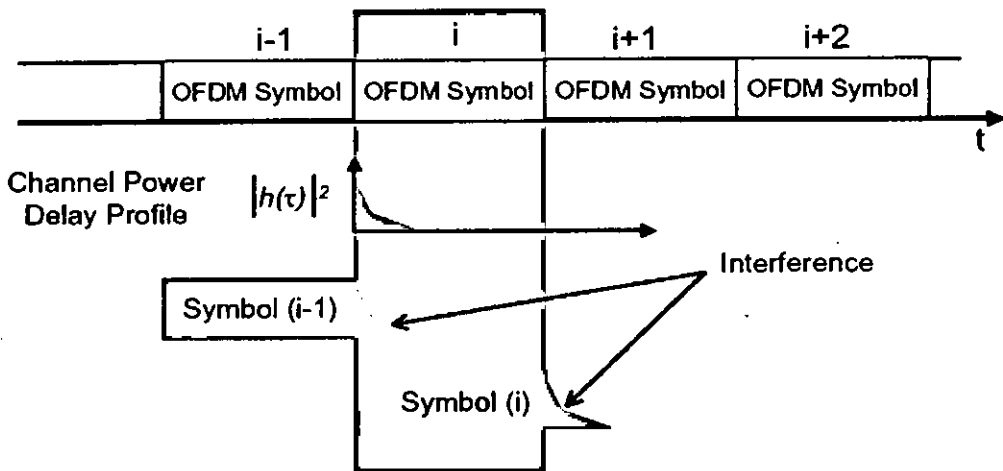
Fig. 2.11(a): Channel delay spread causes ISI between OFDM symbols.
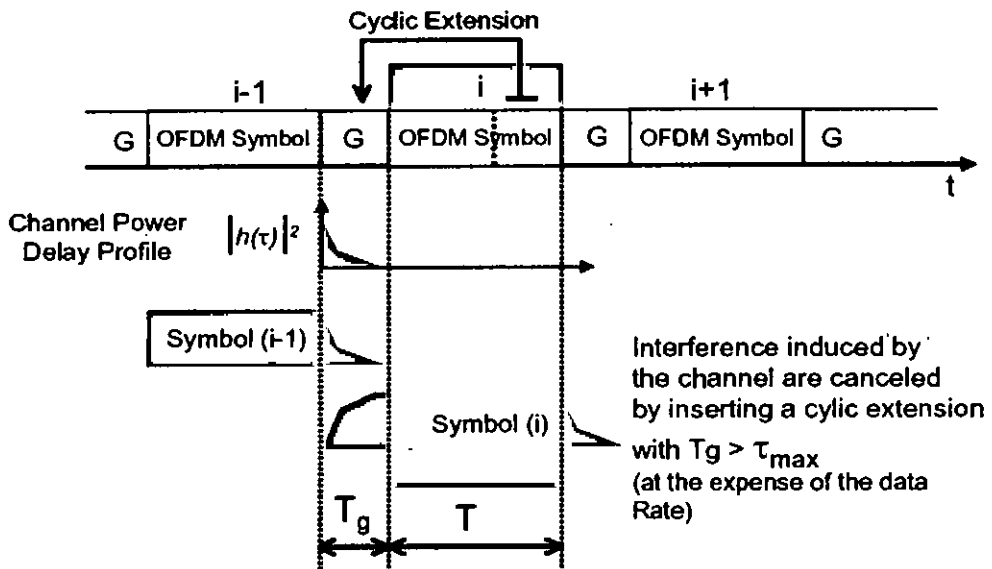
Fig. 2.11(b): Insertion of Cyclic prefix eliminates ISI

2.5.3.5 Baseband to passband conversion

The output of the OFDM modulator generates a base band signal, which must be converted to the required transmission frequency. This can be implemented using analog techniques as shown in Fig 2.12 or using a Digital Up Converter as shown in Fig. 2.13. Both techniques perform the same operation, however the performance of the digital modulation will tend to be more accurate due to improved matching between the processing of the I and Q channels, and the phase accuracy of the digital IQ modulator.
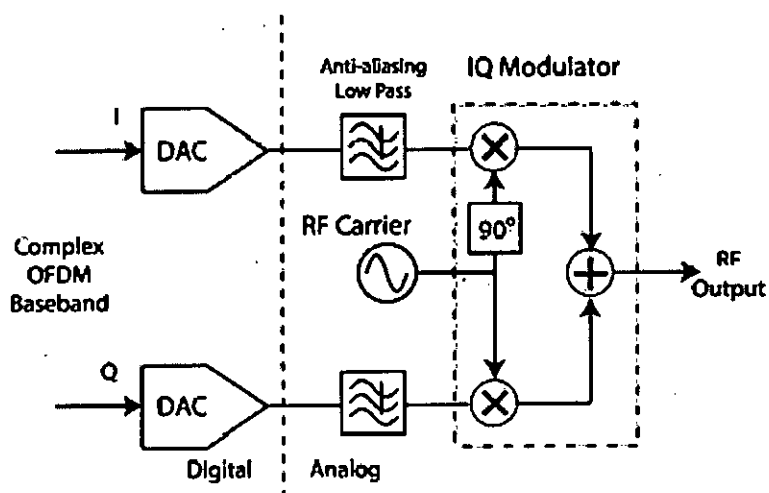
Fig. 2.12: Up conversion of complex base band OFDM signal, using analog techniques
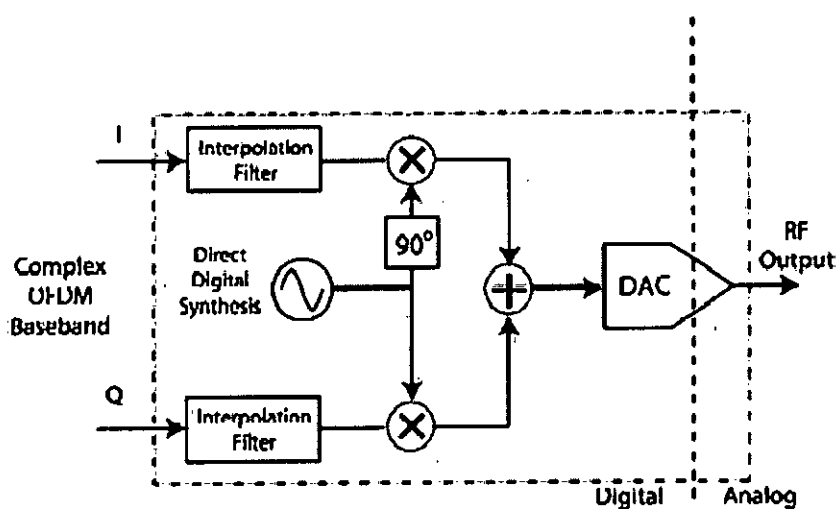
Fig. 2.13: Up conversion of complex base band OFDM signal, using digital techniques.

2.5.4 Bit error rate (BER) expression for OFDM

The BER of an OFDM system is dependent on several factors, such as the modulation scheme, the level of noise in the signal and some other factors that cause ISI and ICI. It is noticeable that the performance of OFDM with just AWGN is exactly the same as that of a single carrier coherent transmission using the same modulation scheme. If we look at a single OFDM subcarrier (since the subcarriers are orthogonal to each other, this does not affect the performance in any way) then this is exactly the same as a single carrier transmission. Thus, the BER expression for an OFDM and single carrier system is identical over AWGN channel and depends only on the channel SNR and modulation level [19]. For BPSK-OFDM the conditional probability of bit error expression is given by [19],

$$P_b(e) = 0.5 \, erfc \, (\sqrt{E_b / N_0})$$
$$= 0.5 \, erfc \, (\sqrt{\gamma_b})$$

(2.9)

where, by definition, γ_b is the SNR per bit.

For any M-ary PSK-OFDM the conditional bit error probability expression is approximated as [14]

$$P_b(e) \approx \frac{1}{k} erfc \, (\sqrt{k \gamma_b} \, \sin \frac{\pi}{M})$$

(2.10)

where, $k = \log_2 M$

2.5.5 Drawbacks of OFDM

1. Very much sensitive to synchronization errors, e.g., carrier frequency offset, phase noise and timing errors.

2. A fast fading channel, i.e., in the case where the channel impulse response varies within the duration of an OFDM symbol, is likely to corrupt the orthogonality between subcarriers. Hence, OFDM is preferred to be implemented in a slow fading channel.

3. Loss in spectral efficiency due to guard interval (GP or CP).

4. The superposition of many subcarriers results in a high peak to average power ratio (PAPR) which is a major drawback in OFDM systems due to the non-linear behavior of power amplifiers (PA). Either the PA is operated with a large back-off factor, or strong peaks of OFDM will drive it into saturation. The resulting clipping effects give rise to ICI and an associated degradation in system performance [22].

Amplitude of an OFDM signal

Amplifier Characteristics
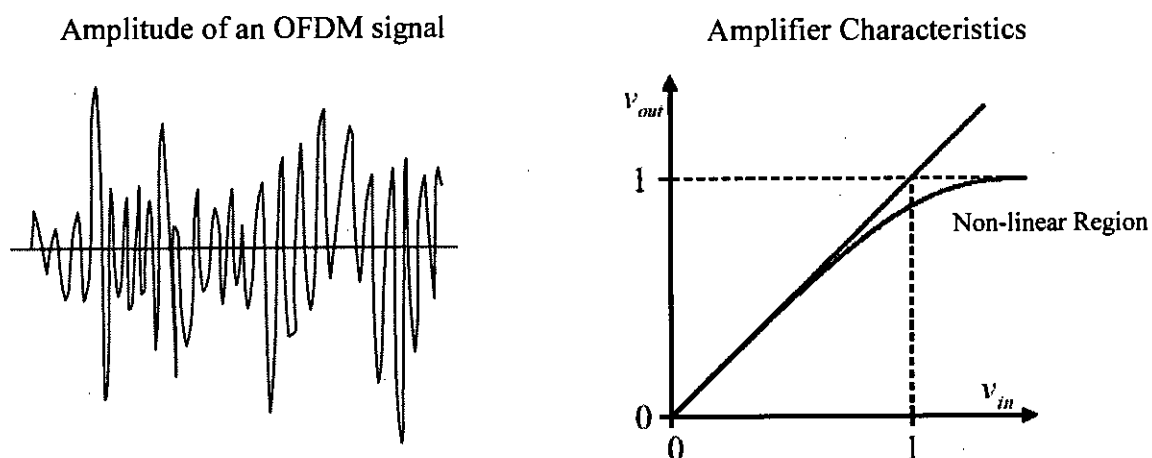
Fig. 2.14: OFDM with large fluctuations in amplitude operates at the non-linear region of a real power amplifier

$$PAPR = \frac{Peak\ Power}{Average\ Power}$$
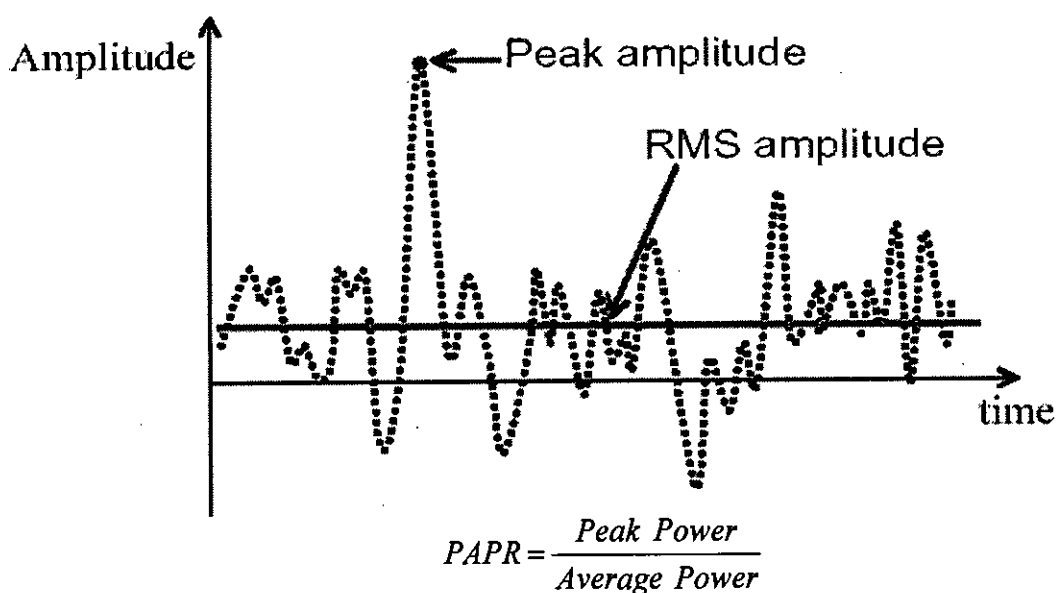
Fig. 2.15: High value of PAPR in OFDM signals

2.6   Synchronization Errors in OFDM

In many wireless communication systems transmitters require a local oscillator (LO) for the up-conversion of the transit baseband signal to a radio frequency (RF) signal (passband signal) and receivers also need a LO for the down conversion. The imperfections of LOs would lead to carrier phase errors. Furthermore, a precise clock signal is required in a digital communication system for symbol synchronization. The process of extracting such a clock signal is called timing recovery [16]. Timing errors would occur either when the clock signal is not correctly recovered, or when the sampling is not performed at the precise sampling instants e.g., in the case that there exists a time delay which is not exactly discovered. In general, these synchronization errors give rise to performance degradation.

In this section we will have a look at the synchronization errors encountered in OFDM briefly. They are normally classified into two categories: carrier phase errors and timing errors.

2.6.1   Carrier phase errors

Let, an OFDM baseband signal $x(n)$ is transmitted over an ideal channel and perfect timing synchronization is available at the receiver, then the carrier phase errors are the only reasons for performance loss. The received signal may be written as

$$y(n) = x(n)e^{(j\theta(n)+\theta_0)} \tag{2.11}$$

where θ_0 represents constant phase offset and $\theta(n)$ is the time variant carrier phase error (CPE). The time variant CPE can result either from the frequency mismatch between oscillators at the transmitter and receiver, f_ε, or from a time variant phase noise, $\varphi(n)$.

Constant phase offset

The constant phase offset, θ_0 is introduced due to the phase mismatch between the transmitter and receiver carrier oscillators. In OFDM transmission, this constant phase offset leads to a rotation over an angle of θ_0 of the OFDM signals on all subcarriers and hence no ISI or ICI is introduced. Such phase offset is carrier-independent and can be compensated at the receiver by multiplying with $e^{-j\theta_0}$

Carrier frequency offset (CFO)

The carrier frequency offset (CFO), f_ε, is the frequency difference between the transmitter and receiver oscillators. CFO arises due to the Doppler shifts introduced by the channel. Let, Δf represent the subcarrier frequency spacing in an OFDM system. The CFO normalized to Δf is denoted by ε. In the presence of CFO, the carrier phase error increase linearly with time: $\theta(n) = 2\pi f_\varepsilon n$. Furthermore, as shown in Fig. 2.16, only when $f_\varepsilon = 0$ and the signal is sampled exactly at subcarrier frequencies, where the peak of a $sinc(x)$ function lies and spectra of other signals have null, no ICI is introduced. A frequency offset would lead to amplitude reduction and phase rotation of the transmitted signal, as well as the ICI from other subcarriers. However, no ISI is introduced by CFO.
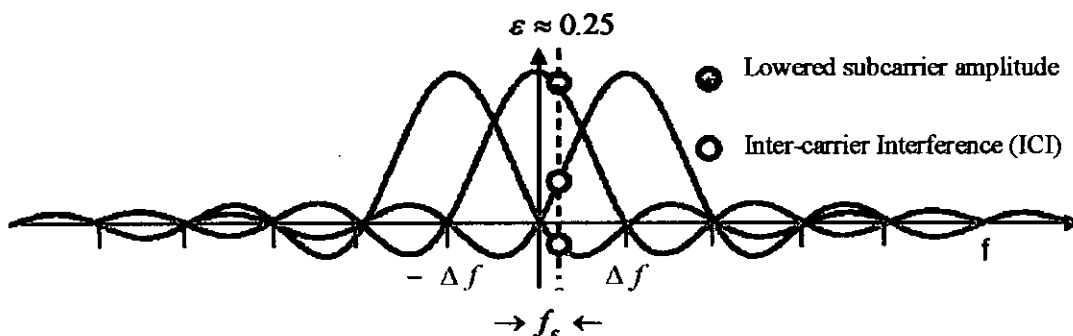
Fig. 2.16:- The effect of Carrier Frequency Offset (CFO)

Phase noise

The time variant phase noise, $\varphi(n)$, is a random process which results from the fluctuation of the transmitter and receiver local oscillators (LO). Assuming a free running LO is used in the receiver, $\varphi(n)$ can be modeled as a Wiener process with zero mean and variance,

$\sigma_u^2 = \dfrac{2\pi\beta T}{N}$, [5], where β denotes the two-sided 3-dB linewidth of the Lorentzian power

density spectrum of the free running LO [8] and T denote OFDM symbol period.

Phase noise has two effects on an OFDM system: rotation of the symbols over all subcarriers by a common phase error (CPE) and the occurrence of ICI [8] as shown in Fig. 2.17.
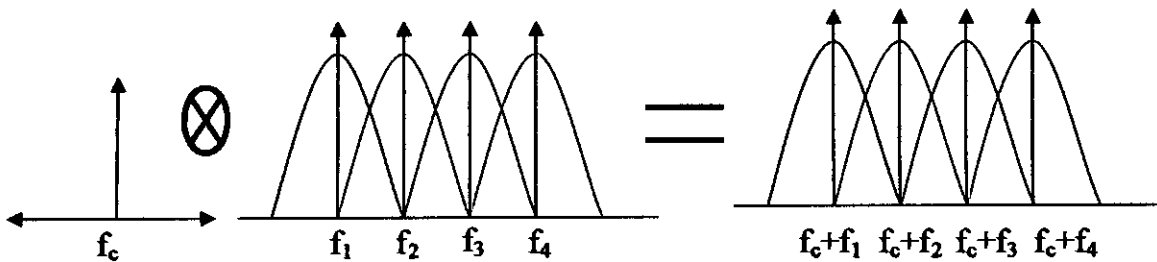
Fig. 2.17(a): Ideal LO: no phase noise effect and hence no ICI.
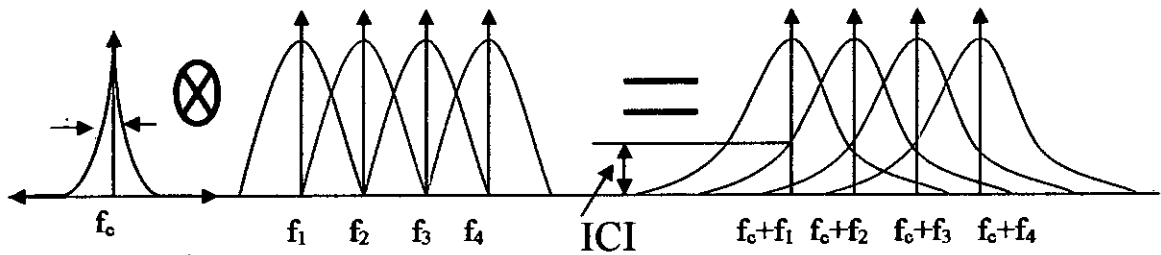
Fig. 2.17(b): Practical LO: introduces ICI due to phase noise effect.

2.6.2 Timing errors

In the ideal world, the duration of a perfectly pulsed signal at a certain frequency level of 1 MHz, for instance, would be exactly 1 μs, with an alternating edge every 500 ns. Such a signal, unfortunately, does not exist. As shown in Fig. 2.18, there are bound to be variations in the length of the period, which causes uncertainty about when the next edge of the signal will occur. This uncertainty is timing jitter. Jitter is a measurement of the variations in the time domain, and essentially describes how far the signal period has wandered from its ideal value.
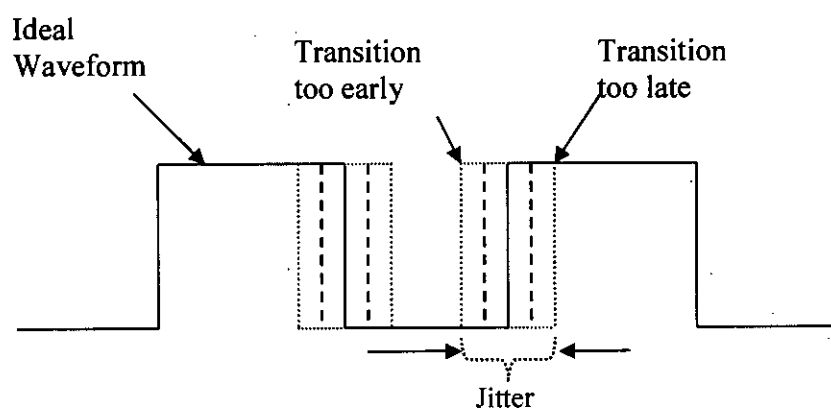
Fig. 2.18: Waveform timing variations causes Jitter

The terminology 'timing jitter' is used to describe the disturbance to an ideal timing signal, and is defined as the time difference between the ideal and the jittered signals as a function of phase. So in the sampling circuit at the receiver additional error may occur in the determination of the best sampling phase. This means that the sampling instants are non-ideal and given by [13]

$$t_n = nT + \xi_n \tag{2.12}$$

where ξ is the timing jitter of the nth sampling instants normalized by symbol duration T.

From Fig. 2.18 we can see that timing jitter (ξ) causes performance degradation of the system by reducing the received energy per bit and on the other hand introducing additional source of additive noise.

2.7   Summary

- Two important features of the wireless radio channels, i.e., multipath propagation and time variance were introduced and their effects on the received signal were discussed in section 2.2. In general, the time variations of the channel appear to be unpredictable to the user. A tapped delay line model was developed for the mathematical description of the channel.

- After the discussion on multiplexing and multiple access techniques, as well as the need for the multicarrier modulation (MCM), OFDM was first introduced in section 2.5. OFDM is a multi-carrier transmission technique which allows a bandwidth efficient data transmission with a low implementation complexity. The attraction of OFDM is mainly due to how the system handles the frequency selective fading and inter-symbol interference (ISI). The basic principle, parameters, properties and drawbacks were explained there.

- A brief overview of synchronization errors encountered in OFDM has been given in section 2.6. They are classified into two groups: carrier phase errors and timing errors. Their influence on OFDM has been introduced concisely. These synchronization impairments cause ICI and BER performance degradation.

CHAPTER 3

INFLUENCE OF CARRIER FREQUENCY OFFSET (CFO), PHASE NOISE AND TIMING JITTER ON UNCODED OFDM SYSTEMS

3.1   Introduction

Many studies have shown that one of the principle disadvantages of OFDM is its sensitivity to synchronization errors, for example, carrier frequency offset (CFO), phase noise and timing jitter [3]-[14]. At the end of the previous chapter a brief overview of synchronization errors encountered in OFDM has been given.

In this chapter, the pure OFDM system model shown in Chapter 2 is modified for the case where CFO, phase noise and timing jitter all three impairments are present. Such a model allows us to analyze the combined effects of CFO, phase noise and jitter on OFDM systems.

The chapter is organized as follows. In Section 3.2, OFDM system model is given in a practical scenario considering the effect of channel, imperfect local oscillator (LO) and non-ideal sampling circuit of the receiver. To analyze the combined effect of synchronization errors, mathematical modeling of channel, CFO, phase noise and timing jitter are given. Then in Section 3.3, theoretical analysis is presented for evaluating the performance of an uncoded OFDM under the combined influence of CFO, phase noise and timing jitter over Rayleigh fading channels. Finally an exact closed form expression for the Signal-to-Interference-plus-Noise Ratio (SINR) and the average bit error rate (BER) is derived for uncoded OFDM systems considering the effect of these three impairments.

3.2   System Model

Consider the mth symbol, $x_m(n)$, of an N-subcarrier OFDM system is transmitted over Rayleigh fading channel. Doppler shifts of the channel causes frequency difference

between the transmitter and receiver oscillators and introduces CFO (f_ε) in the system which is characterized in Fig. 3.1. At the down conversion stage, the imperfect local oscillator (LO) is modeled by an ideal LO with the effect of phase noise, $\varphi_m(n)$. Finally in the A/D circuit, the non-ideal nature of sampler is characterized by timing jitter ξ_n, as shown in Fig. 3.1.
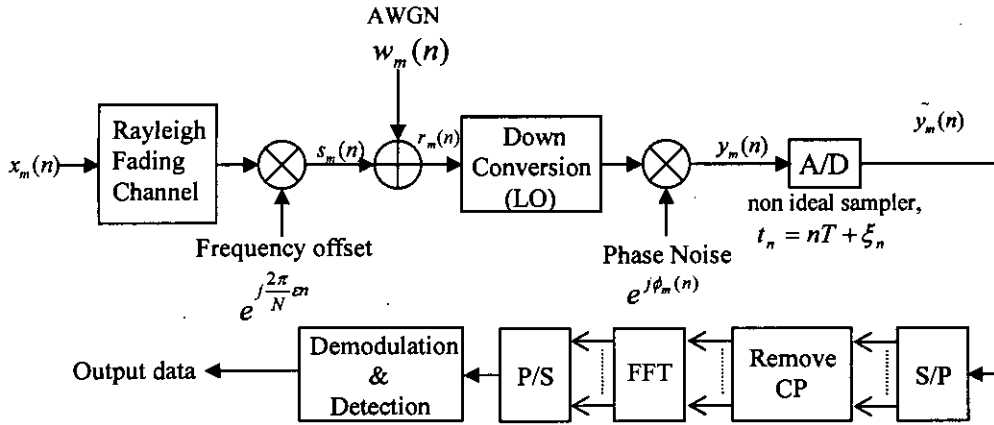
Fig. 3.1: OFDM system model (receiver) in the presence of CFO, phase noise and timing jitter over Rayleigh channel

To analyze the combined effects of CFO, phase noise and jitter in the given system model, at first, mathematical models of channel, CFO, phase noise and timing jitter will be developed respectively in the following sections.

3.2.1 Channel model

The most popular radio channel model is the so called discrete multipath time-domain model extensively discussed in chapter 2. The multipath channel is modeled as a linear filter and it is assumed to be a slow varying channel whose response does not vary within an OFDM symbol. The channel impulse response (CIR) can be expressed as

$$h(\tau) = \sum_{r=0}^{M-1} h_r \delta(\tau - \tau_r) \tag{3.1}$$

where M, h_r and τ_r are the number of paths, the complex-valued path gain and time delay of the r-th path, respectively, and $\delta(x)$ is a Dirac delta function. Delay spread $\{\tau_r\}_{r=0}^{M-1}$ is uniformly and independently distributed within $[0, N_g]$ with N_g denoting the cyclic prefix length. For a wide sense stationary uncorrelated scattering (WSSUS) channel, h_r can be modeled as an independent zero-mean complex Gaussian random variable due to the central limit theorem. Then $|h_r|$ follows a Rayleigh distribution and $|h_r|^2$ is exponentially distributed [16]. For the mth symbol of an N-subcarrier OFDM system, the corresponding channel gains in frequency domain are expressed by $\{H_m(k)\}_{k=0}^{N-1}$ satisfying the condition $E[|H_m(k)|^2] = 1$ with $E[g]$ denoting the ensemble average of the variable g.

The multipath fading channel can be characterized by the power-delay profile and the exponential power-delay profile can be approximately written as [29]

$$E[|h_r|^2] = e^{-cr} \tag{3.2}$$

where c stands for the channel decay constant.

3.2.2 Carrier frequency offset (CFO) model

The carrier frequency offset (CFO), f_ε, arises due to the Doppler shifts introduced by the channel which causes frequency difference between the transmitter and receiver oscillators. The absolute value of f_ε, $|f_\varepsilon|$, is either an integer multiple or a fraction of the subcarrier frequency spacing, Δf, or the sum of them. If normalizing f_ε to the subcarrier spacing Δf, the resulting normalized CFO of the channel in general can be expressed as

$$\varepsilon = \frac{f_\varepsilon}{\Delta f} = \delta + \in \tag{3.3}$$

where δ is an integer and $|\in| \leq 0.5$.

The influence of an integer CFO on OFDM system is different from the influence of a fractional CFO. In the event that $\delta \neq 0$ and $\varepsilon = 0$, symbols transmitted on a certain subcarrier, e.g., subcarrier k, will shift to another subcarrier k_δ,

$$k_\delta = k + \delta \bmod N - 1.$$ (3.4)

If δ is unknown at the receiver, then information cannot be recovered from the received symbols such that the resulting BER will be 0.5. Nonetheless, no ICI is caused by an integer CFO. As we focus on the ICI effect we will consider only the normalized CFO, $\varepsilon = \dfrac{f_\varepsilon}{\Delta f} = \in$ and from now CFO will be denoted by ε. We assume CFO (ε) to be a Gaussian process statistically independent of the input signal with zero mean and variance σ_ε^2.

3.2.3 Phase noise model

The time variant phase noise, $\varphi(t)$, is a random process which results from the fluctuation of the transmitter and receiver local oscillators (LO). Assuming a free running LO is used in the receiver, $\varphi(t)$ can be modeled as a continuous path Brownian motion (or Wiener process) with zero mean and variance, $2\pi\beta|t|$, [5]; where β denotes the two-sided 3-dB linewidth of the Lorentzian power density spectrum of the free running LO [8] .

Phase noise on the mth symbol of an OFDM system, $\varphi_m(n)$, can be modeled as [5]

$$\varphi_m(n) = \varphi_{m-1}(N-1) + \sum_{i=-N_g}^{n} u[m(N+N_g)+i] = \sum_{i=0}^{m(N+N_g)+N_g+n} u(i) = C_m + \sum_{i=0}^{n} u(T_m+i)$$ (3.5)

where C_m and T_m are defined by

$$C_m = \sum_{i=0}^{m(N+N_g)+N_g-1} u(i) \text{ and } T_m = m(N+N_g)+N_g$$ (3.6)

N_g is the length of cyclic prefix and $u(i)$'s denote mutually independent Gaussian random variables with zero mean and variance $\sigma_u^2 = \dfrac{2\pi\beta T}{N} = \dfrac{2\pi\beta}{R}$, where T and R denote the OFDM symbol period transmission data rate respectively.

3.2.4 Timing jitter model

In the sampling circuit (A/D) at the receiver additional error may occur in the determination of the best sampling phase. This means that the sampling instants are non-ideal and given by [13]

$$t_n = nT + \xi_n \tag{3.7}$$

where ξ is the timing jitter of the nth sampling instants normalized by symbol duration T. Timing jitter can be modeled as a stationary Gaussian random process statistically independent of the input signal with zero mean and variance σ_ξ^2 [6].

3.3 Analysis of the Combined Effect of CFO, Phase Noise and Timing Jitter

The transmitted OFDM signal for the mth symbol is given by the N point complex modulation sequence

$$x_m(n) = \sum_{k=0}^{N-1} X_m(k) e^{j\frac{2\pi}{N}nk} \tag{3.8}$$

where n ranges from 0 to $N + N_g - 1$.

As shown in Fig. 3.1, the received signal, $r_m(n)$ considering multipath fading, AWGN noise and the effect of CFO can be expressed as

$$\begin{aligned} r_m(n) &= [\sum_{k=0}^{N-1} X_m(k) e^{j\frac{2\pi}{N}nk}] \times [H_m(k) e^{j\frac{2\pi}{N}n\varepsilon}] + w_m(n) \\ &= [\sum_{k=0}^{N-1} X_m(k) H_m(k) e^{j\frac{2\pi}{N}n(k+\varepsilon)}] + w_m(n) \end{aligned} \tag{3.9}$$

In (3.9) $H_m(k)$ is the transfer function of the channel at the frequency of the kth carrier and $w_m(n)$ is the complex envelope of AWGN with zero mean and variance σ^2.

After down conversion at the imperfect LO, the received signal $y_m(n)$ (shown in Fig. 3.1) is affected by phase noise and can be modeled as

$$y_m(n) = r_m(n) e^{j\varphi_m(n)} \tag{3.10}$$

Since phase noise does not change the AWGN noise energy, $w_m(n)$ can be separated from $r_m(n)$ and (3.10) can be modified as

$$y_m(n) = s_m(n)e^{j\varphi_m(n)} + w_m(n) \tag{3.11}$$

where, $s_m(n) = \sum_{k=0}^{N-1} X_m(k)H_m(k)e^{j\frac{2\pi}{N}n(k+\varepsilon)}$.

Assuming $\varphi_m(n)$ is small [10], so that

$$e^{j\varphi_m(n)} \approx 1 + j\varphi_m(n) \tag{3.12}$$

Substituting (3.12) into (3.11) then yields

$$y_m(n) = s_m(n) + s_m(n)j\varphi_m(n) + w_m(n) \tag{3.13}$$

After DFT and by dropping the subscript 'm' (3.13) yields

$$Y(k) = S(k) + S(k) \otimes j\Theta(k) + W(k) \tag{3.14}$$

where, $S(k)$, $\Theta(k)$ $W(k)$ are the DFT responses of $s_m(n)$ $\varphi_m(n)$, and $w_m(n)$ respectively and $\otimes$ denotes the circular convolution operation.

Now, $S(k)$ is given by,

$$
\begin{aligned}
S(k) &= \frac{1}{N}\sum_{n=0}^{N-1}[\sum_{k=0}^{N-1} X(k)H(k)e^{j\frac{2\pi}{N}n(k+\varepsilon)}]e^{-j\frac{2\pi}{N}nk} \\
&= \sum_{n=0}^{N-1}\frac{1}{N}[X(k)H(k)e^{j\frac{2\pi}{N}n(k+\varepsilon)} + \sum_{\substack{r=0 \\ r\neq k}}^{N-1} X(r)H(r)e^{j\frac{2\pi}{N}n(r+\varepsilon)}]e^{-j\frac{2\pi}{N}nk}
\end{aligned}
\tag{3.15}
$$

Therefore, $S(k)$ consists of two components, signal component and interference and is given by: $S(k) = S_1(k) + I_1(k)$

where, $$S_1(k) = \frac{1}{N}X(k)H(k)\sum_{n=0}^{N-1}e^{\frac{j2\pi n\varepsilon}{N}} \tag{3.16}$$

Now,

$$\sum_{n=0}^{N-1}e^{\frac{j2\pi n\varepsilon}{N}} = (e^{\frac{j2\pi\varepsilon}{N}})^0 + (e^{\frac{j2\pi\varepsilon}{N}})^1 + (e^{\frac{j2\pi\varepsilon}{N}})^2 + \cdots \quad \cdots + (e^{\frac{j2\pi\varepsilon}{N}})^{N-1} \tag{3.17}$$

$$= \frac{(e^{\frac{j2\pi\varepsilon}{N}})^N - 1}{(e^{\frac{j2\pi\varepsilon}{N}}) - 1}$$

$$\sum_{n=0}^{N-1} e^{\frac{j2\pi n\varepsilon}{N}} = \frac{1-(e^{\frac{-j2\pi\varepsilon}{N}})^N}{1-(e^{\frac{-j2\pi\varepsilon}{N}})} \times \frac{e^{j2\pi\varepsilon}}{e^{j2\pi\varepsilon/N}}$$

$$= \frac{1-(e^{\frac{-j2\pi\varepsilon}{N}})^N}{1-(e^{\frac{-j2\pi\varepsilon}{N}})} \times e^{j2\pi\varepsilon(\frac{N-1}{N})}$$

$$= \frac{\sin(\pi\varepsilon)}{\sin(\frac{\pi\varepsilon}{N})} \times e^{-j\pi\varepsilon(\frac{N-1}{N})} \times e^{j2\pi\varepsilon(\frac{N-1}{N})}$$

$$= \frac{\sin(\pi\varepsilon)}{\sin(\frac{\pi\varepsilon}{N})} \times e^{j\pi\varepsilon(\frac{N-1}{N})}$$

Therefore,

$$S_1(k) = \frac{1}{N} X(k)H(k) \sum_{n=0}^{N-1} e^{\frac{j2\pi n\varepsilon}{N}} = X(k)H(k) \frac{\sin(\pi\varepsilon)}{N\sin(\frac{\pi\varepsilon}{N})} e^{j\pi\varepsilon(\frac{N-1}{N})} \qquad (3.18)$$

The first component, $S_1(k)$ is the modulation value $X(k)$ modified by the channel transfer function, $H(k)$. Equation (3.18) shows that $S_1(k)$ experiences an amplitude reduction and phase shift due to CFO,(ε). As N is always much greater than ($\pi\varepsilon$), $N\sin(\frac{\pi\varepsilon}{N})$ is replaced by ($\pi\varepsilon$). Assuming $E[X_k] = 0$ and $E[X_k X_l^*] = |X|^2 \delta_{lk}$ and average channel gain $E\{|H_l|^2\} = |H|^2$ we obtain

$$E[|S_1(k)|^2] = |X|^2 |H|^2 \sin c^2(\pi\varepsilon) \qquad (3.19)$$

The second term is the ICI caused only by the CFO and is given by

$$I_1(k) = \frac{1}{N}\sum_{\substack{r=0\\r\neq k}}^{N-1} X(r)H(r)\sum_{n=0}^{N-1} e^{\frac{j2\pi n\varepsilon}{N}} = \sum_{\substack{r=0\\r\neq k}}^{N-1} X(r)H(r)\frac{\sin(\pi\varepsilon)}{N\sin(\frac{\pi(r-k+\varepsilon)}{N})}e^{j\pi\varepsilon(\frac{N-1}{N})}e^{-j\pi(\frac{r-k}{N})}$$

$$(3.20)$$

$E[|I_1(k)|^2]$ is evaluated in (Appendix-I) as

$$E[|I_1(k)|^2] \leq 0.5947|X|^2|H|^2(\sin\pi\varepsilon)^2; \qquad |\varepsilon| \leq 0.5 \qquad (3.21)$$

In (3.14) the second term, $S(k)\otimes j\Theta(k)$ gives the joint effect of phase noise and CFO. Let,

$$I_2(k) = S(k)\otimes j\Theta(k)$$

$$= \{\frac{1}{N}\sum_{n=0}^{N-1}[\sum_{k=0}^{N-1} X(k)H(k)e^{j\frac{2\pi}{N}n(k+\varepsilon)}]e^{-j\frac{2\pi}{N}nk}\}\otimes j\Theta(k)$$

$$= [\frac{1}{N}\sum_{k=0}^{N-1} X(k)H(k)\sum_{n=0}^{N-1}e^{j\frac{2\pi}{N}n\varepsilon}]\otimes j\Theta(k)$$

$$= [\sum_{k=0}^{N-1} X(k)H(k)\frac{\sin(\pi\varepsilon)}{N\sin(\frac{\pi\varepsilon}{N})}e^{j\pi\varepsilon(\frac{N-1}{N})}]\otimes j\Theta(k); \quad from\,(3.17)$$

So the ICI term due to joint effects of phase noise and CFO is given by

$$I_2'(k) = j\sum_{\substack{r=0\\r\neq k}}^{N-1} X(r)H(r)\frac{\sin(\pi\varepsilon)}{N\sin(\frac{\pi\varepsilon}{N})}e^{j\pi\varepsilon(\frac{N-1}{N})}\Theta(k-r) \qquad (3.22)$$

In (Appendix-II) the energy of $\Theta(r)$ is given by,

$$E[|\Theta(r)|^2] = \frac{\sigma_u^2}{2N\sin^2(\frac{\pi r}{N})} \qquad (3.23)$$

Thus $E[|I_2'(k)|^2]$ can be evaluated as

$$E[|I_2'(k)|^2] = |X|^2|H|^2\sin c^2(\pi\varepsilon)\frac{\sigma_u^2}{2N\sum_{r=1}^{N-1}\sin^2(\frac{\pi r}{N})} \qquad (3.24)$$

As channel SNR γ is defined by, $\gamma = \dfrac{|X|^2 |H|^2}{E[|W(k)|^2]} = \dfrac{E_c}{N_0}$, where E_c is the averaged received

energy of the individual carriers and $\dfrac{N_0}{2}$ is the power spectral density of the AWGN and

we have used the condition $E[|H(k)|^2] = 1$ given in section 3.2.1. Therefore the *SINR*

expression due to a combined effect of CFO and phase noise may be expressed as

$$SINR(\varepsilon, \sigma_u^2) \geq \frac{\gamma\{\sin c^2(\pi\varepsilon)\}}{1 + \gamma[0.5947(\sin \pi\varepsilon)^2 + \{\dfrac{\sigma_u^2}{2N}\sin c^2(\pi\varepsilon)\displaystyle\sum_{r=1}^{N-1}\dfrac{1}{\sin^2(\dfrac{\pi r}{N})}\}]} \quad ; \quad |\varepsilon| \leq 0.5 \quad (3.25)$$

Note that for a slow fading channel of section 3.2.1, given $H(k)$, we can reach a conclusion

that the *SINR* expression for multipath channels in (3.25) has the same form as for the

AWGN channels, if transmitted signals are independent and channel energy on each

subcarrier is unity.

The individual effect of CFO and phase noise can be easily obtained from (3.25) as

$$SINR(\varepsilon) \geq \frac{\gamma\{\sin c^2(\pi\varepsilon)\}}{1 + \gamma[0.5947(\sin \pi\varepsilon)^2]} \quad ; \quad |\varepsilon| \leq 0.5 \quad ; \quad \sigma_u^2 = 0 \quad (3.26)$$

$$SINR(\sigma_u^2) \geq \frac{\gamma}{1 + \gamma\{\dfrac{\sigma_u^2}{2N}\displaystyle\sum_{r=1}^{N-1}\dfrac{1}{\sin^2(\dfrac{\pi r}{N})}\}} \quad ; \quad |\varepsilon| = 0 \quad (3.27)$$

In the non-ideal sampling circuit, the amplitude of the samples is affected by a random

timing jitter (ξ) which ultimately causes the averaged received energy of the individual

carriers, E_c to degrade by a factor of $(1-\xi)$ over a time slot and on the other hand it

increases additive noise energy by $E_c\xi$. So in the presence of timing jitter along with CFO

and phase noise the *SINR* expression of (3.25) is modified as follows

$$SINR(\varepsilon,\sigma_u^2,\xi) \geq \cfrac{\gamma(1-\xi)\{\operatorname{sinc}^2(\pi\varepsilon)\}}{1+\gamma(1-\xi)[0.5947(\sin\pi\varepsilon)^2 + \{\cfrac{\sigma_u^2}{2N}\operatorname{sin}c^2(\pi\varepsilon)\sum_{r=1}^{N-1}\cfrac{1}{\sin^2(\cfrac{\pi r}{N})}\}]+\gamma\xi} ; \quad |\varepsilon| \leq 0.5 ; |\xi| \leq 1$$

(3.28)

(3.28) indicates that, in the presence of CFO, phase noise and timing jitter, several parameters affect OFDM system performance, resulting in severe performance degradation which is unacceptable in practice. In the absence of frequency offset ($\varepsilon = 0$) the *SINR* expression of (3.28) reduces to

$$SINR(\sigma_u^2,\xi) \geq \cfrac{\gamma(1-\xi)}{1+\gamma(1-\xi)[\{\cfrac{\sigma_u^2}{2N}\sum_{r=1}^{N-1}\cfrac{1}{\sin^2(\cfrac{\pi r}{N})}\}]+\gamma\xi} ; \quad |\xi| \leq 1 \qquad (3.29)$$

which indicates the combined effect of phase noise and timing jitter. In the case of perfect carrier-phase synchronization, $\Theta(r)$ becomes a Dirac delta function and σ_u^2 approaches zero, while the *SINR* expression of (3.29) reduces to

$$SINR(\xi) \geq \frac{\gamma(1-\xi)}{1+\gamma\xi} \quad |\xi| \leq 1 \qquad (3.30)$$

Finally for an ideal sampling circuit ($\xi = 0$) and *SINR* expression of (3.30) becomes channel SNR, γ .

From the SINR expression of (3.28), the conditional probability of bit error, $P_b(e\,|\,\varepsilon,\xi)$ for a BPSK-OFDM system, conditioned on a given value of ε and ξ for a given channel SNR, γ and phase noise variance, σ_u^2 can be obtained from (2.9) as

$$P_b(e\,|\,\varepsilon,\xi) = 0.5\,erfc(\sqrt{SINR(\varepsilon,\xi)}) \qquad (3.31)$$

Similarly from (2.10) the conditional probability of bit error, $P_b(e\,|\,\varepsilon,\xi)$ for any M-ary PSK-OFDM system under the combined influence of CFO, phase noise and timing jitter can be approximated as

$$P_b(e \mid \varepsilon, \xi) \approx \frac{1}{k} erfc\left(\sqrt{k\,SINR(\varepsilon,\xi)}\sin\frac{\pi}{M}\right) \tag{3.32}$$

where $k = \log_2 M$.

The unconditional or the average BER for OFDM systems can be calculated by averaging the conditional probability of bit error over all possible values of ε and ξ as

$$BER = \int\limits_{-\infty}^{\infty}\int\limits_{-\infty}^{\infty} P_b(e \mid \varepsilon, \xi)\, p(\varepsilon)\, p(\xi)\, d\varepsilon\, d\xi \tag{3.33}$$

Since ε and ξ are assumed Gaussian processes, the probability density functions (PDFs) $p(\varepsilon)$ and $p(\xi)$ are Gaussian and given by,

$$p(\varepsilon) = \frac{1}{\sqrt{2\pi\sigma_\varepsilon^2}} \times \exp(-\varepsilon^2 / 2\sigma_\varepsilon^2) \tag{3.34}$$

$$p(\xi) = \frac{1}{\sqrt{2\pi\sigma_\xi^2}} \times \exp(-\xi^2 / 2\sigma_\xi^2) \tag{3.35}$$

3.4 Summary

- In this chapter, we have analyzed the combined effects of CFO, phase noise and timing jitter on OFDM systems. The OFDM system model have been modified for the practical scenario where CFO, phase noise and timing jitter all three impairments are present.

- The derivation of an exact closed form expression for the Signal-to-Interference-plus-Noise Ratio (SINR) for the system model is one of the most important contributions in this work. The combined effects of CFO, phase noise and timing jitter are exhibited by expressing the OFDM system BER performance as a function of its critical parameters. The SINR and BER expression for the system shows that in the presence of all three synchronization impairments, several parameters affect OFDM system performance, resulting in severe performance degradation which is unacceptable in practice.

CHAPTER 4

PERFORMANCE IMPROVEMENT TECHNIQUES:
TURBO CODING & DIVERSITY

4.1   Introduction

From the analysis of the SINR and BER expressions of the last chapter we have found that uncoded OFDM system suffers severe performance degradation under the combined influence of CFO, phase noise and timing jitter. This chapter deals with the performance improvement techniques for uncoded OFDM with or without synchronization impairments.

The chapter is organized as follows. In Section 4.2 the need for coding and diversity techniques in OFDM is explained briefly with a simple example. The OFDM system model of Chapter 3 is extended with turbo coder in Section 4.3. After a brief description of turbo encoder and decoder, the BER performance with turbo codes is analyzed. Finally, the selection criteria of turbo code parameters for the system operating at different SNR region are explained in this section. OFDM system with diversity techniques is discussed in Section 4.4. After a brief overview of the combining methods used for multiple antenna systems, the BER performance with antenna diversity using maximal-ratio combiner is evaluated.

4.2   Need for Coding and Diversity

Uncoded OFDM does not perform well in frequency selective channels [23], since a characteristic of frequency selective fading is that some frequencies are enhanced whereas others are attenuated. As a result, subcarriers with poor SNR will dominate the performance of the system. An extreme example is the channel with 0dB echo (accordingly the existence of null subcarrier). As an example, in Fig. 4.1, the frequency response of a

two path channel with **h** = [1, 1] in an OFDM system with 64 subcarriers are demonstrated. It can be seen that the transfer function of subcarrier 41 equals zero.
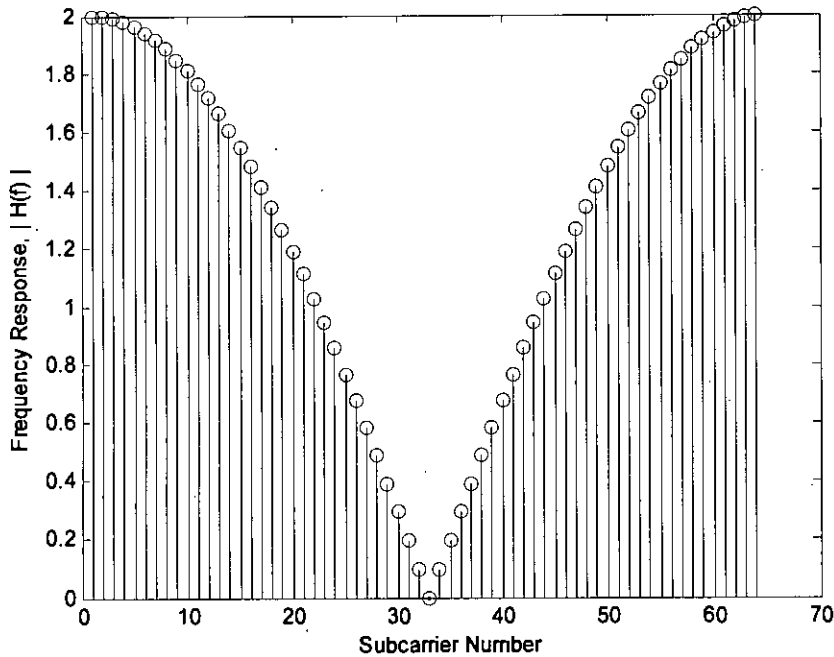
Fig. 4.1: Frequency selective fading

Information transmitted on this subcarrier will be lost if the transmission is uncoded, and therefore average BER tends to be $\dfrac{1}{2} \times \dfrac{1}{64}$ as SNR approaches infinity. Thus error correction coding is expected to be implemented in practical OFDM systems to cope with the problems of multipath reception. The resulting system is so-called coded OFDM (COFDM). COFDM is able to deliver an acceptable BER at a reasonably low SNR [19]. In addition, interleaving is utilized as well to reduce the risk of successively receiving faded out signals when assigning successive symbols to adjacent subcarriers.

Another technique to deal with frequency selective behavior is diversity transmission. If we can supply to the receiver several replicas of the same information signal transmitted over independent fading channels, the probability that all the signal components will fade simultaneously is reduced considerably. A commonly used method for achieving diversity

employs multiple antennas [28]. The performance improvement through coding and diversity are discussed in the following sections.

4.3   System Model with Turbo Coding

To see the effect of error correction and coding technique, a coder block is added with the OFDM system under synchronization impairments. As turbo codes outperform the most powerful codes known to date [24] and more importantly they are much simpler to decode, turbo codes are chosen in this section. A complete coded-OFDM (COFDM) block diagram is shown in Fig. 4.2.
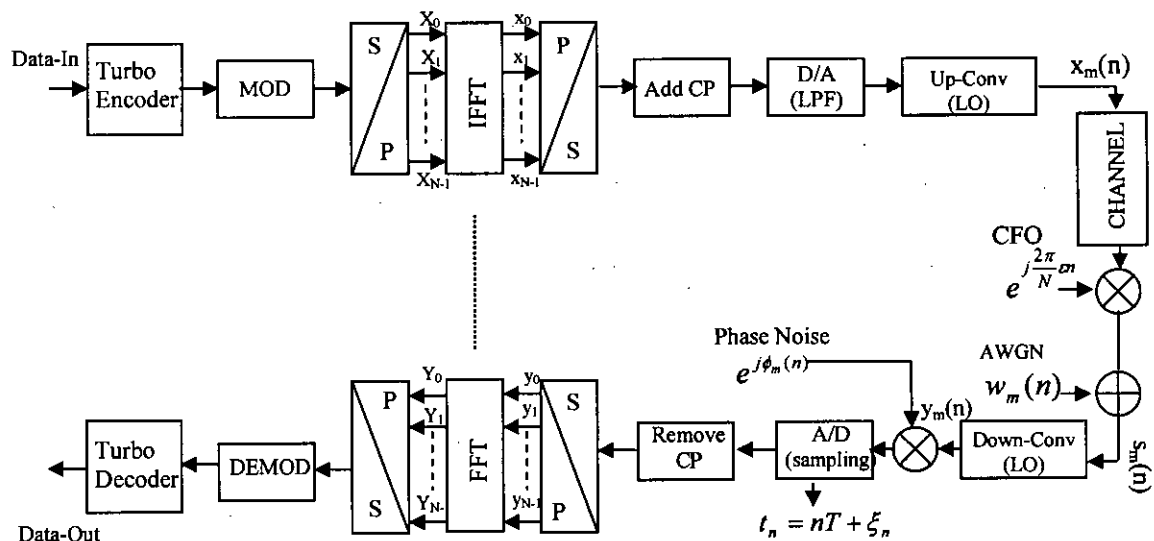
Fig. 4.2: A complete OFDM system model with turbo coding in the presence of CFO, phase noise and timing jitter

As the function of all the blocks are discussed in details in the previous chapters, we will concentrate only on the turbo coder block in this section.

4.3.1 Turbo encoder & decoder

A turbo encoder is a combination of two simple recursive systematic convolutional (RSC) encoders, each using a small number of states. For a block of k information bits, each constituent code generates a set of parity bits and so the code rate of the encoder is 1/3. The turbo code consists of the information bits and both sets of parity, as shown in Fig. 4.3. The generator matrix of a rate ½ component RSC code can be represented as

$$G(D) = [1 \quad \frac{g_1(D)}{g_0(D)}]$$ where $g_0(D)$ and $g_1(D)$ are feedback and feed-forward polynomials

with degree v, respectively.

The key innovation is an interleaver P, which permutes the original k information bits before encoding the second code. If the interleaver is well-chosen, information blocks that correspond to error-prone codewords in one code will correspond to error-resistant codewords in the other code. The resulting code achieves performance similar to that of Shannon's random codes [24]. However, random codes approach optimum performance only at the price of a prohibitively complex decoder.
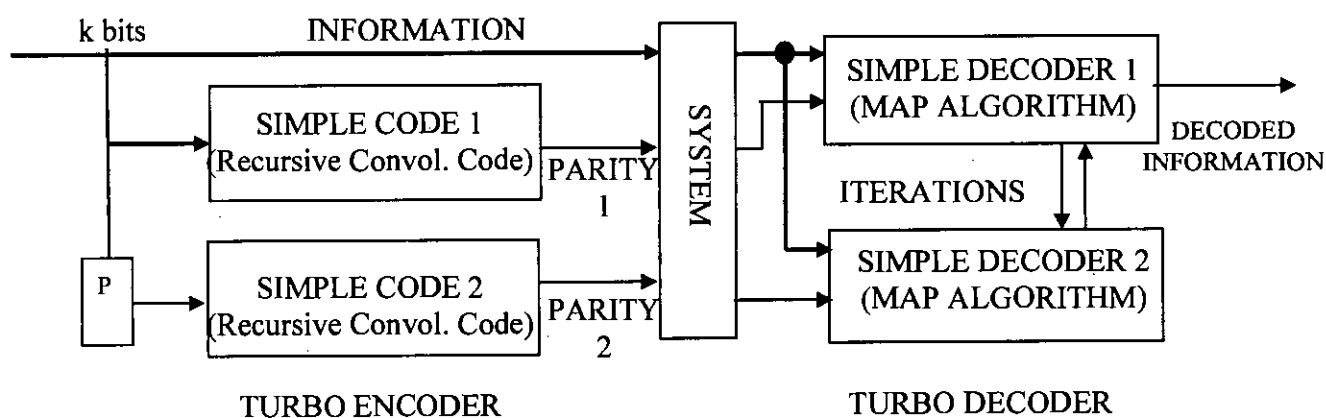
Fig. 4.3: Structure of turbo encoder and decoder

Turbo decoding uses two simple decoders individually matched to the simple constituent codes. Each decoder sends likelihood estimates of the decoded bits to the other decoder,

and uses the corresponding estimates from the other decoder as a priori likelihoods. The constituent decoders use the "MAP" (maximum a posteriori) bitwise decoding algorithm, which requires the same number of states as the well-known Viterbi algorithm. The turbo decoder iterates between the outputs of the two decoders until reaching satisfactory convergence. The final output is a hard-quantized version of the likelihood estimates of either of the decoders.

4.3.2 Asymptotic BER performance analysis of turbo codes

The hamming weight of a code word is the total number of non-zero components in the code word. The minimum free distance of a code is defined as the smallest hamming distance between two different codewords in the code. The linearity property of the codes implies that the minimum distance of the code is the smallest weight of the nonzero codewords in the code. The importance of the minimum free distance parameter is in the fact that it determines the error correcting and detecting capability of a code.

At high SNR's the asymptotic BER probability of turbo codes is dominated by the code minimum free distance and is given by [25]

$$P_{b_{TC}}(e) \cong \frac{1}{2} B_d erfc(\sqrt{d_f C_R \gamma_b}) \tag{4.1}$$

where B_d (known as error coefficients) is the average number of ones on the minimum free distance path in the overall turbo code trellis, d_f is the code minimum free distance, C_R is the code rate and γ_b is the SNR per bit. Eq. (4.1) defines the asymptotic behavior of turbo codes.

The value of d_f depends on the generator polynomials and the interleaver structure. For a uniform interleaver and the 16-state rate 1/3 code with the generator polynomials $g_0 = (47)$ and $g_1 = (21)$ the value of d_f is 9. As this value of d_f is relatively low, the curve defined by (4.1) has a very low slope at high SNR's, which is often referred to as the "error floor".
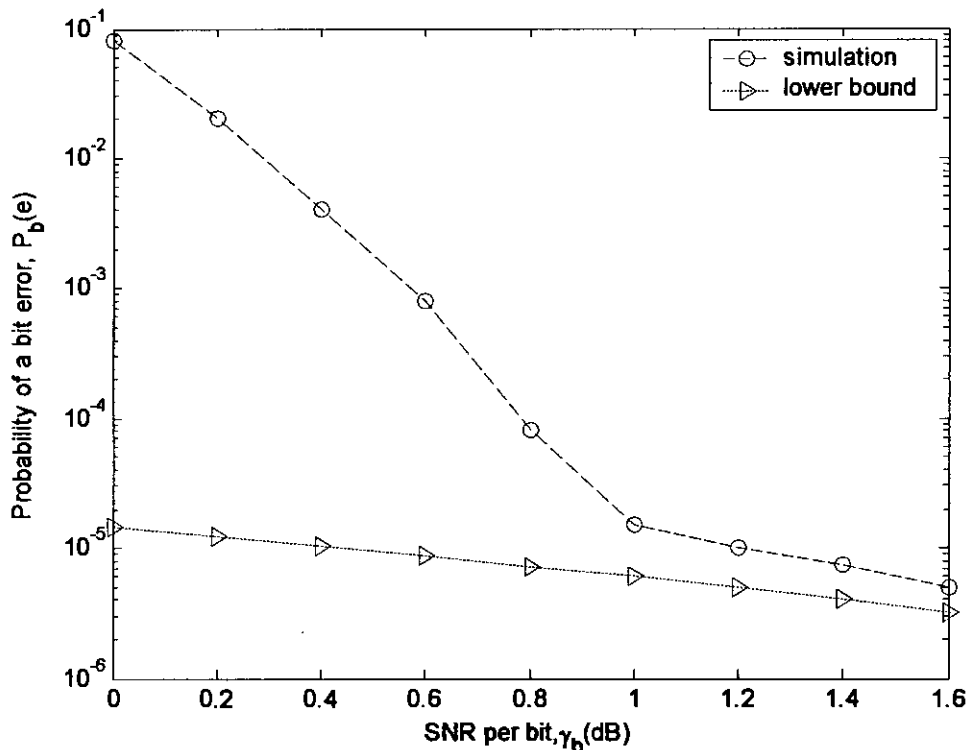
Fig. 4.4: Simulation result and theoretical bound of turbo codes with rate 1/3, memory order 4 and interleaver size 1024 on AWGN channels.

The simulation results for this code on an AWGN channel, interleaver size 1024 and 10 iterations along with the theoretical bound in (4.1) are shown in Fig. 4.4. It is clear that the lower bound in (4.1) closely determines the code performance at high SNR's.

In this section, turbo code performance is discussed based on the asymptotic bounds of the BER probability. In the next section, we evaluate turbo code BER performance based on distance spectrum and its average upper bounds.

4.3.3   BER performance upper bounds for turbo codes

For small interleaver sizes (20 and 50), the code distance spectrum (d_f, B_d) [25] is given in Table 4.1.

Table 4.1

Code Distance Spectrum

Turbo encoder : memory order, v =2 Interleaver size, P=20			Turbo encoder : memory order, v =2 Interleaver size, P=50	
Code free distance, d_f	Error coefficient, B_d		Code free distance, d_f	Error coefficient, B_d
7	0.04		7	7.05e-3
8	0.01		8	7.45e-4
9	0.22		9	0.04
10	0.26		10	0.08
16	8.30		11	0.12
17	12.35		12	0.18
18	25.04		14	0.27
19	37.02		14	0.39
-	-		28	3.18e+2
-	-		29	6.11e+2
-	-		40	1.05e+3
-	-		41	1.72e+3
-	-		42	2.93e+3

The BER probability upper bound can be expressed based on the code distance spectrum by [25]

$$P_{b_{TC}}(e) \le \frac{1}{2} \sum_{d=d_{free}} B_d \, erfc(\sqrt{d_f \, C_R \, \gamma_b}) \qquad (4.2)$$

The effect of distance spectrum on BER probability can be explained by comparing the (d_f, B_d) values of Table-4.1 for turbo codes with interleaver sizes 20 and 50. In the low to medium region of distances, error coefficients for the code with interleaver size, P = 50 are lower than those for the code with interleaver size, P = 20. However, for large distances, the error coefficients for the code with P = 50 are higher. In spite of this, the code with P =

50 has better performance than the code with P = 20 in the medium to high SNR region as shown in Fig. 4.5. This property remains invariant for various codes. Consequently, we can conclude that only error coefficients at low to medium distances are significant for error performance.
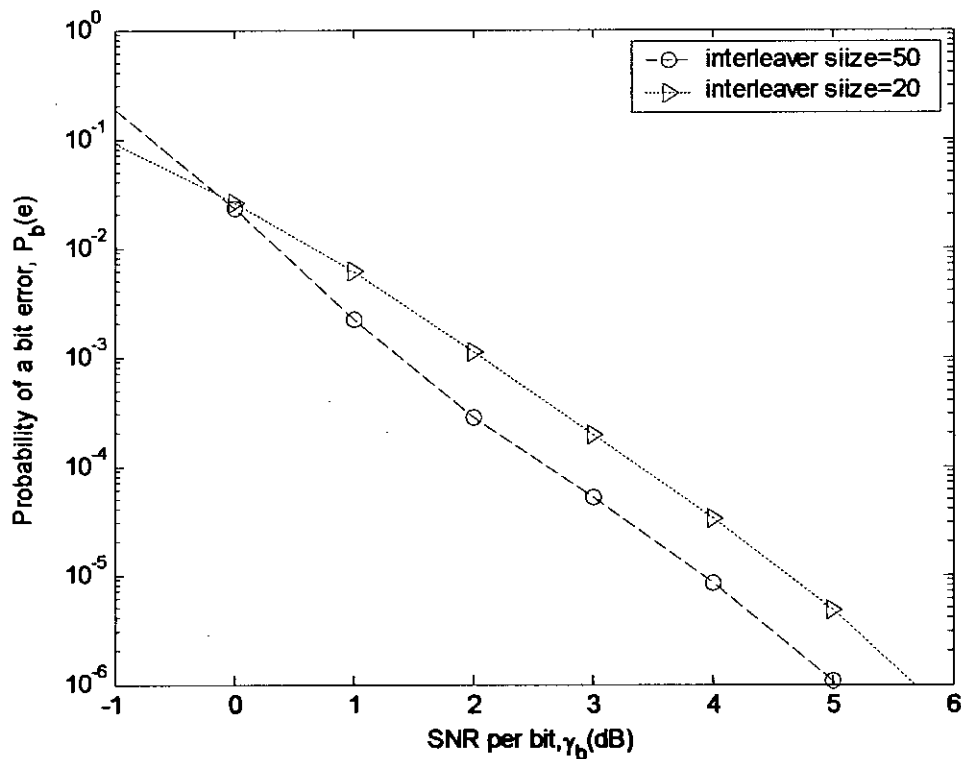
Fig. 4.5: BER probability upper bounds for turbo code with interleaver sizes of 20 and 50

4.3.4 BER performance analysis for turbo coded-OFDM with synchronization errors

In chapter-3, the SINR expression (3.28) for uncoded OFDM considering the combined influence of CFO, phase noise and jitter is derived as

$$SINR(\varepsilon, \sigma_u^2, \xi) \geq \frac{\gamma(1-\xi)\{\sin c^2(\pi\varepsilon)\}}{1+\gamma(1-\xi)[0.5947(\sin \pi\varepsilon)^2 + \{\frac{\sigma_u^2}{2N}\sin c^2(\pi\varepsilon)\sum_{r=1}^{N-1}\frac{1}{\sin^2(\frac{\pi r}{N})}\}]+\gamma\xi} \quad ; \quad |\varepsilon| \leq 0.5 \ ; |\xi| \leq 1$$

From the analysis of section 4.3.2 and 4.3.3, the asymptotic BER probability and the BER probability upper bounds for a turbo-coded BPSK-OFDM system with synchronization impairments may be expressed respectively as

$$P_{b_{TC}}(e \mid \varepsilon, \xi) \approx \frac{1}{2} B_d erfc(\sqrt{d_f \ C_R SINR(\varepsilon, \xi)}) \qquad (4.3)$$

$$P_{b_{TC}}(e \mid \varepsilon, \xi) \leq \frac{1}{2} \sum_{d=d_{free}} B_d erfc(\sqrt{d_f \ C_R \ SINR(\varepsilon, \xi)}) \qquad (4.4)$$

where, C_R , B_d and d_f are the code rate, error co-efficient and code free distance respectively.

Similarly, for any turbo coded M-ary PSK OFDM system, the asymptotic BER probability and the BER probability upper bounds can be expressed respectively as

$$P_{b_{TC-Mary}}(e \mid \varepsilon, \xi) \approx \frac{1}{2k} B_d erfc(\sqrt{d_f \ C_R \times kSINR(\varepsilon, \xi)} \sin(\frac{\pi}{M})) \qquad (4.5)$$

$$P_{b_{TC}}(e \mid \varepsilon, \xi) \leq \frac{1}{2k} \sum_{d=d_{free}} B_d erfc(\sqrt{d_f \ C_R \times k \ SINR(\varepsilon, \xi)} \sin(\frac{\pi}{M})) \qquad (4.6)$$

Finally, the average BER for turbo-coded OFDM systems can be calculated by averaging the conditional probability of bit error over all possible values of ε and ξ as

$$BER = \int_{-\infty}^{\infty} \int_{-\infty}^{\infty} P_{b_{TC}}(e \mid \varepsilon, \xi) \, p(\varepsilon) \, p(\xi) \, d\varepsilon \, d\xi \qquad (4.7)$$

4.3.5 Analysis on turbo code parameter selection

From equations (4.1) - (4.6), one can see that the code free distance d_f and error coefficients B_d affect the turbo code error performance considerably. From Fig. 4.6, it is clear that the average BER of turbo codes at low SNR is dominated by error coefficients. On the other hand, code effective free distance mainly dominates the code performance at

high SNRs. Obviously the code design criteria depend on the region of SNR's where the code is used. A turbo code performing well in the region of high SNR's may not perform well in the region of low SNR's and vice-versa. Thus, good turbo codes should be designed according to the range of SNR's where the code is used. The BER probability corresponding to high SNR is below 10^{-5} and BER probability corresponding to low SNR is in the range of $10^{-1} \sim 10^{-5}$.
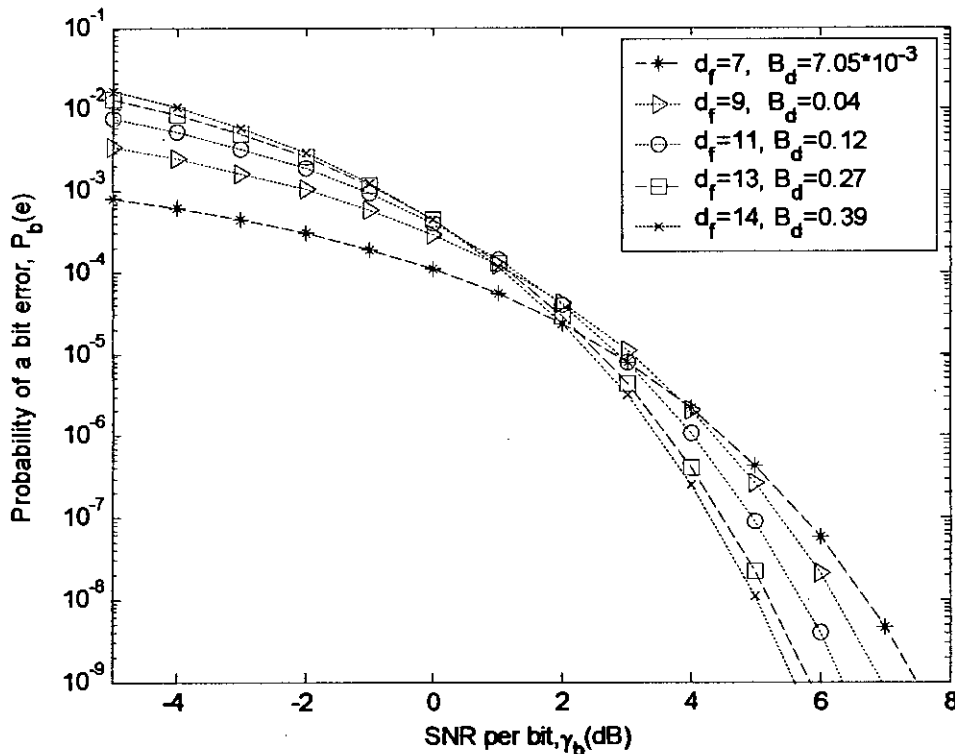
Fig. 4.6: Performance of turbo codes with rate 1/3 and memory order 2 on AWGN channels for different code free distance and error coefficients

Maximizing the code effective free distance can be used as the design criterion for constructing good turbo codes at high SNR's when inter-leaver size becomes large [26]. The above objective was applied to find good rate 1/3 Benedetto-Montorsi (BM) turbo codes using rate 1/2 RSC component codes (Table-4.2).

For a fixed effective free distance, optimizing the BER probability implies minimization of the error coefficients. However, a non-maximum effective free distance can have an optimal distance spectrum (minimum error coefficient) and better performance at low SNR's [27]. The optimal distance spectrum (ODS) turbo codes have minimum BER probability at low SNR's (Table-4.3).

Table 4.2

Best rate 1/3 turbo codes (BM Codes) at high SNR's [26]

Memory order, v	Feedback polynomial, $g_0(D)$	Feed-forward polynomial, $g_1(D)$	Code effective free distance, $d_{f,\mathit{eff}}$	Code free distance, d_f	Input weight, w_f
1	3	2	4	4	2
2	7	5	10	7	3
3	15	17	14	8	4
4	31	33	22	9	5
4	31	27	22	9	5
5	51	77	38	10	6
5	51	67	38	12	4

Table 4.3

Rate 1/3 ODS turbo codes at low SNR's [27]

Memory order, v	Feedback polynomial, $g_0(D)$	Feed-forward polynomial, $g_1(D)$	Code effective free distance, $d_{f,\mathit{eff}}$	Code free distance, d_f
2	7	5	10	7
3	15 (13)	17	14	8
4	37	21	10	9
5	43	55	30	11

Comparing ODS turbo codes with BM codes shown in Table-4.2, one can observe that for memory orders 2 and 4, the BM codes are the same as ODS codes. However, the BM codes do not have the optimal distance spectrum for memory orders larger than 4. For memory orders 4 and 5, a turbo code with a non-maximum effective free distance can have an optimal distance spectrum and better performance at low SNR's.

Increasing the memory order (or, number of shift registers) of component RSC codes generally results in increased free distance and effective free distance. As these two parameters determine the turbo code performance at high SNR's, increasing memory order will give the improved asymptotic error performance. At low SNR's, the performance of turbo codes is dominated by error coefficients which are generally higher for codes with higher memory orders. However, increasing the interleaver size reduces the error coefficients in the same proportion, and thus the effective free distance becomes the dominant parameter at lower SNR than the previous case. For an interleaver size of 1024 bits, the memory order 4 code outperforms the memory order 2 and 4 codes for SNR above 1.5dB. [25]. Higher memory orders are more complex to decode, and seem to offer negligible performance improvement. Constituent codes with memory orders less than 4 may sometimes be desirable to achieve higher decoding speeds with some sacrifice of performance.

4.4   System Model with Diversity Reception

Another technique to deal with frequency selective behavior is diversity transmission. Diversity techniques are based on the notion that errors occur in reception when the channel attenuation in large, i.e., when the channel is in deep fade. If we can supply to the receiver several replicas of the same information signal transmitted over independent fading channels, the probability that all the signal components will fade simultaneously is reduced considerably. That is, if p is the probability that any one signal will fade below some critical value, then p^L is the probability that all L independently fading replicas of the same channel will fade below the critical level. There are several ways in which we can

provide the receiver with L independently fading replicas of the same information bearing signal.

A commonly used method for achieving diversity employs multiple antennas [28]. For example, we may employ a single transmitting antenna and multiple receiving antennas. The later must be spaced sufficiently far apart that the multipath components in the signal have significantly different propagation delays at the antennas. Usually a separation of a few wavelengths is required between two antennas in order to obtain signals that fade independently.
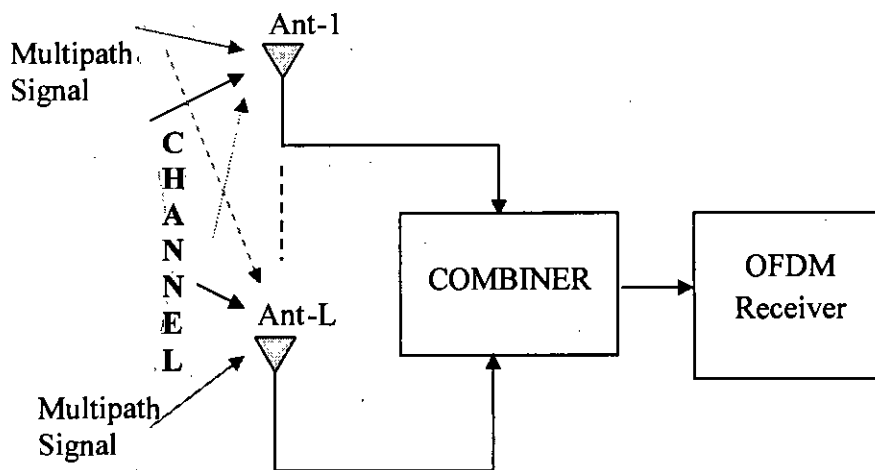
Fig. 4.7: OFDM system with receiver antenna diversity

4.4.1 Methods for combining signals

The methods for combining or selecting uncorrelated faded signals obtained from different antennas are usually classified into the following three categories:

1. Maximal-ratio-combining
2. Equal-gain combining
3. Selection

Block diagrams of three combining methods are shown in Fig 4.8

Fig. 4.8 (a): Maximal-ratio combining (MRC) method

Fig. 4.8 (b): Equal-gain combining method
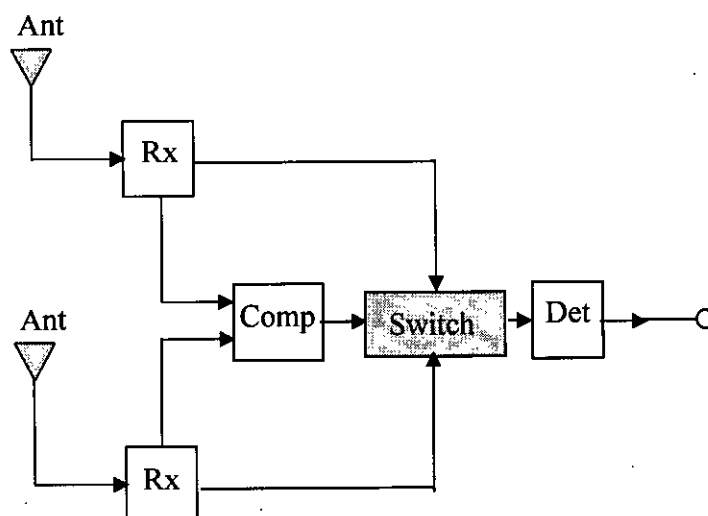
Fig. 4.8 (c): Selection method

Assuming ideal operation, maximal-ratio combining achieves the best performance improvement as compared to the other methods. However, it requires co-phasing, weighting and summing circuits as shown in Fig. 4.8 (a), making the implementation very complicated.

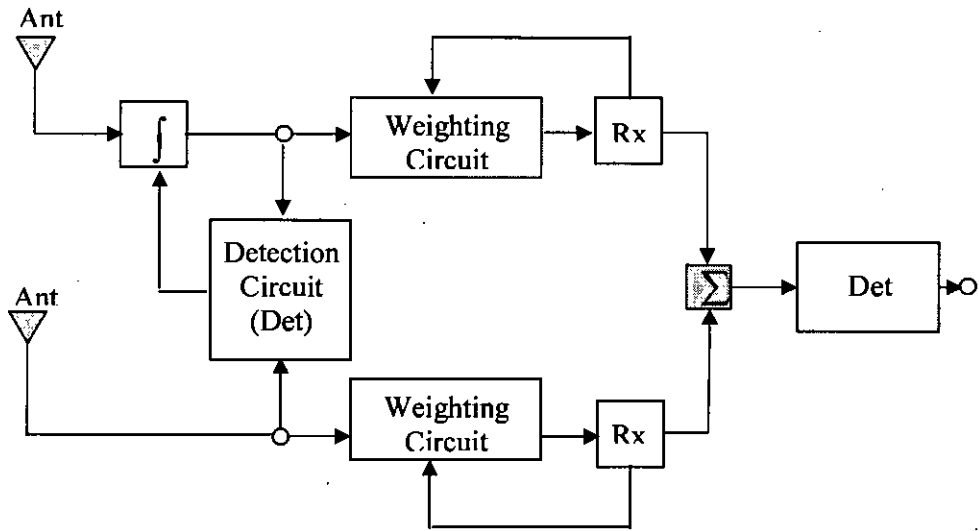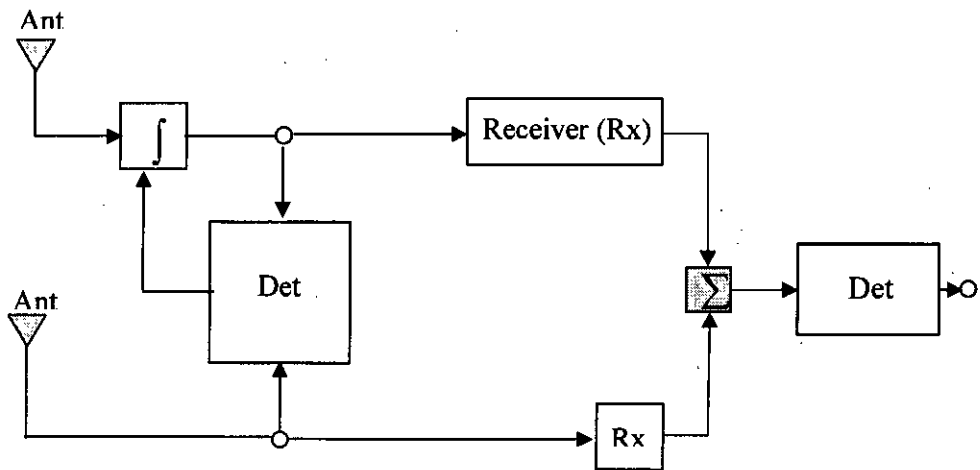Fig. 4.8 (b), shows an equal-gain combining system diagram. It is quite similar to the maximal-ratio combining, except that the weighting circuits are omitted. The performance improvement obtained by an equal-gain combiner is slightly inferior to that of maximal-ratio combiner, since interference and noise corrupted signals may be combined with high quality (noise and interference free) signals.

Selection method is sometimes more suitable because of its simple implementation. In this method, the antenna that captures the highest signal level (or, in more advanced implementations, the branch having the lowest BER) is selected (Fig. 4.8 (c)).

4.4.2 BER performance analysis with diversity

To evaluate the BER performance improvement, first of all, we assume that there are L diversity channels carrying the same information bearing signal. Each channel is assumed

to be slowly fading with Rayleigh-distributed envelope statistics. The fading process among the L diversity channels is assumed to be mutually statistically independent.

If average SNR per diversity branch (or, channel), $\bar{\gamma_c}$ satisfies the condition $\bar{\gamma_c} \gg 1$ (greater than 10dB), then the conditional probability of bit error for BPSK-OFDM with L-diversity branch using maximal ratio combining (MRC) method can be approximated as [28]

$$P_b(e) \approx \left(\frac{1}{4\bar{\gamma_c}} \right)^L \binom{2L-1}{L};$$

(4.8)

where $\binom{2L-1}{L} = \frac{(2L-1)!}{L!(L-1)!}$ and average SNR per bit, $\bar{\gamma_b} = L\bar{\gamma_c}$
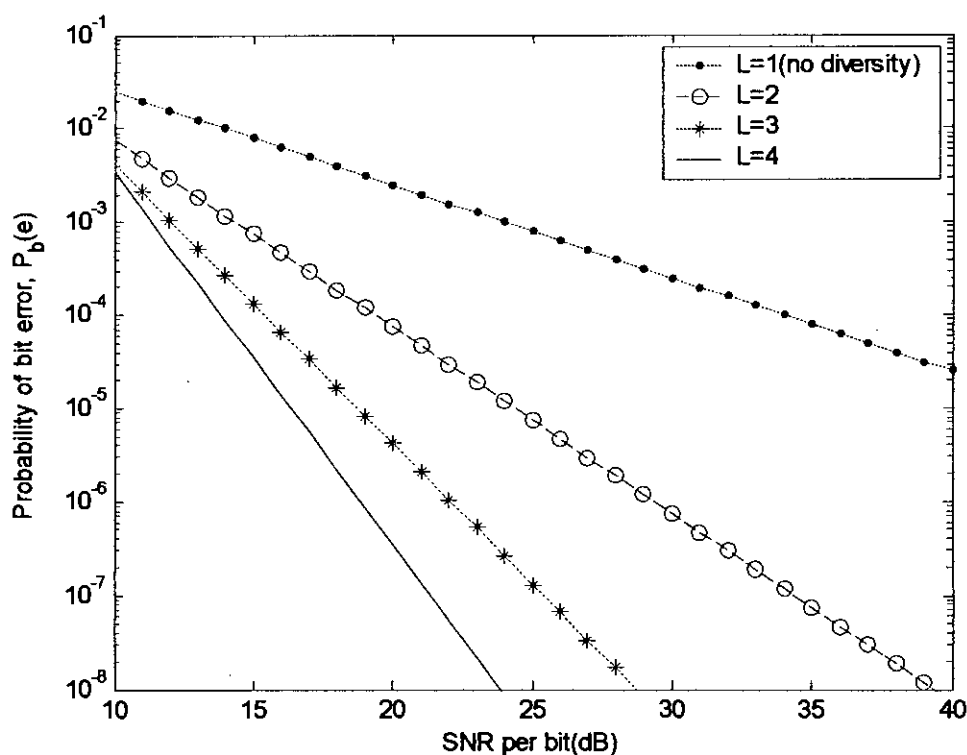

Fig. 4.9: Performance of BPSK-OFDM signals with antenna diversity reception

From the SINR expression of (3.28), the conditional probability of bit error for BPSK-OFDM in the presence of CFO, phase noise and timing jitter with L-diversity branch using maximal ratio combining (MRC) method can be approximated as in (4.8)

$$P_{b_D}(e \mid \varepsilon, \xi) \approx \left(\frac{1}{4\overline{SINR(\varepsilon, \xi)}} \right)^L \binom{2L-1}{L} \tag{4.9}$$

where, $\overline{SINR(\varepsilon, \xi)}$ is the average SINR per diversity branch.

Finally, the average BER for turbo-coded OFDM systems can be calculated by averaging the conditional probability of bit error over all possible values of ε and ξ as

$$BER = \int\limits_{-\infty}^{\infty} \int\limits_{-\infty}^{\infty} P_{b_D}(e \mid \varepsilon, \xi) \, p(\varepsilon) \, p(\xi) \, d\varepsilon \, d\xi \tag{4.10}$$

4.5 Summary

- After explaining the need for coding and diversity for uncoded OFDM, the performance improvement through turbo coding was analyzed in section-4.3. From the asymptotic behavior and the upper bound of BER, wee see that code free distance (d_f) and error coefficients (B_d) affect the turbo code error performance considerably. The values of the distance spectrum (d_f, B_d) also depend on interleaver size and code rate. It is clear that the average BER of turbo codes at low SNR is dominated by error coefficients. On the other hand, code effective free distance mainly dominates the code performance at high SNRs. So a turbo code performing well in the region of high SNR's may not perform well in the region of low SNR's and vice-versa. Increasing the memory order of component codes generally results in increased free distance and effective free distance. As a result, increasing memory order will give the improved asymptotic error performance. However, higher memory orders are more complex to decode, and seem to offer negligible performance improvement. Constituent codes with memory orders less

than 4 may sometimes be desirable to achieve higher decoding speeds with some sacrifice of performance.

- The BER performance with diversity was analyzed in section 4.4. Multiple receiver antennas can provide several replicas of the same information signal to the receiver, transmitted over independent fading channels and the probability that all the signal components will fade simultaneously is reduced considerably. To recover the desired signal from the antennas maximal-ratio-combining is used as it is the best combining technique. Such a system provides the greatest resistance to fading but since the all the receive paths must remain energized, it is also consumes the most power.

CHAPTER 5

RESULTS AND DISCUSSION

5.1 Introduction

In the presence of CFO, phase noise and timing jitter over Rayleigh fading channels, the SINR and BER expressions derived in previous chapters are functions of these three impairments as well as some critical system parameters.

The chapter is organized as follows. In Section 5.2, performance results are illustrated and analyzed for the uncoded OFDM system model developed in Chapter 3. The performance improvement results through turbo coding are discussed in Section 5.3. Finally Section 5.3 reveals the performance results for OFDM with diversity reception.

For the convenience of the readers, the parameters used for computation in this chapter are shown in Table 5.1.

Table 5.1: System Parameters

No. of Subcarriers (N)	1024
Cyclic Prefix Length (N_g)	64
Modulation	BPSK
Data Rate(R)	64/7 MHz
Channel type	Rayleigh fading
SNR	20 dB

5.2   Performance Results for Uncoded OFDM

Fig. 5.1, 5.2 and 5.3 illustrates the individual effect of CFO, timing jitter and phase noise respectively on the BER performance of a BPSK- OFDM system over Rayleigh fading channel. It can be seen from the figures that the BER performance degradation with the increase of the individual variances of σ_s^2, σ_u^2 and σ_ξ^2 respectively. From these figures we can say that the system performance is more sensitive to phase noise variance than CFO and timing jitter as the BER degradation is the highest for phase noise among the three for a much smaller variance than CFO and jitter.

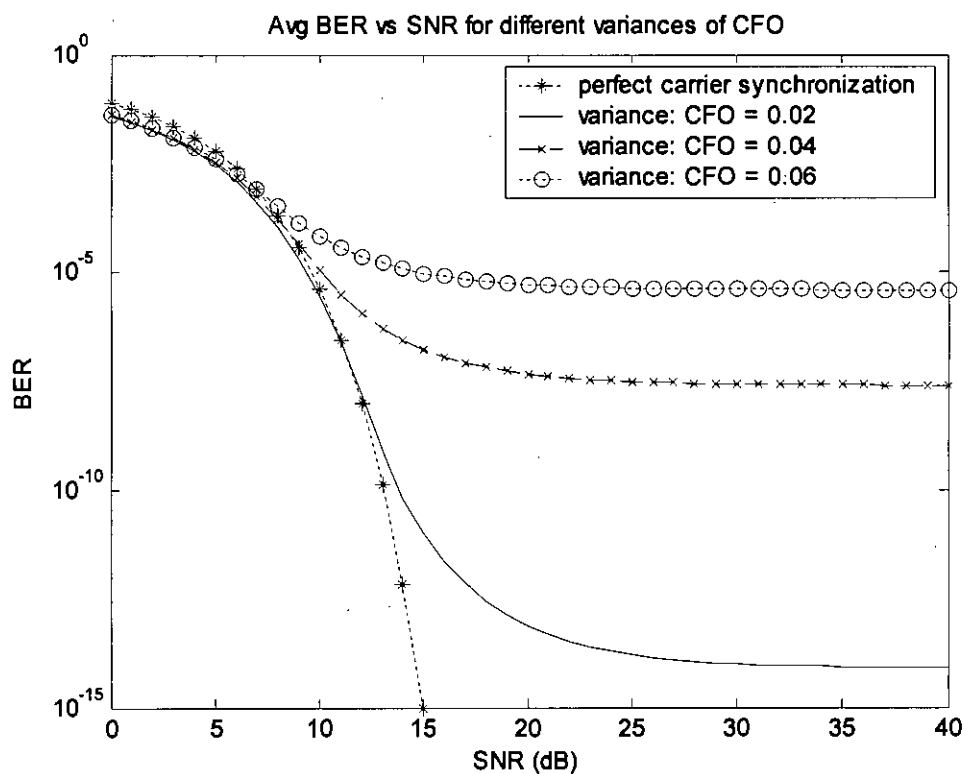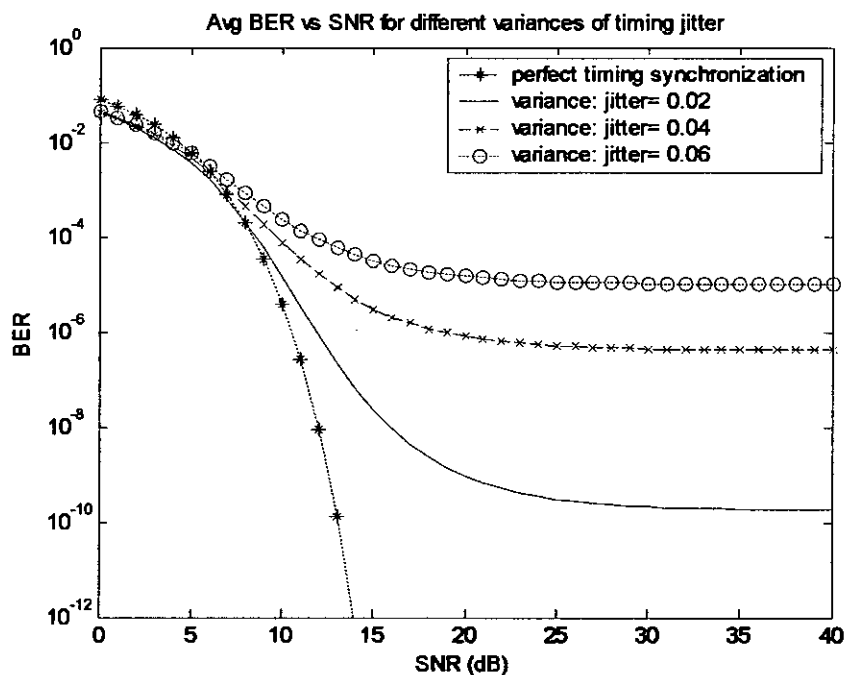**Fig. 5.1:** BER performance of a BPSK-OFDM for different variances of CFO

Fig. 5.2: BER performance of a BPSK-OFDM for different variances of timing jitter
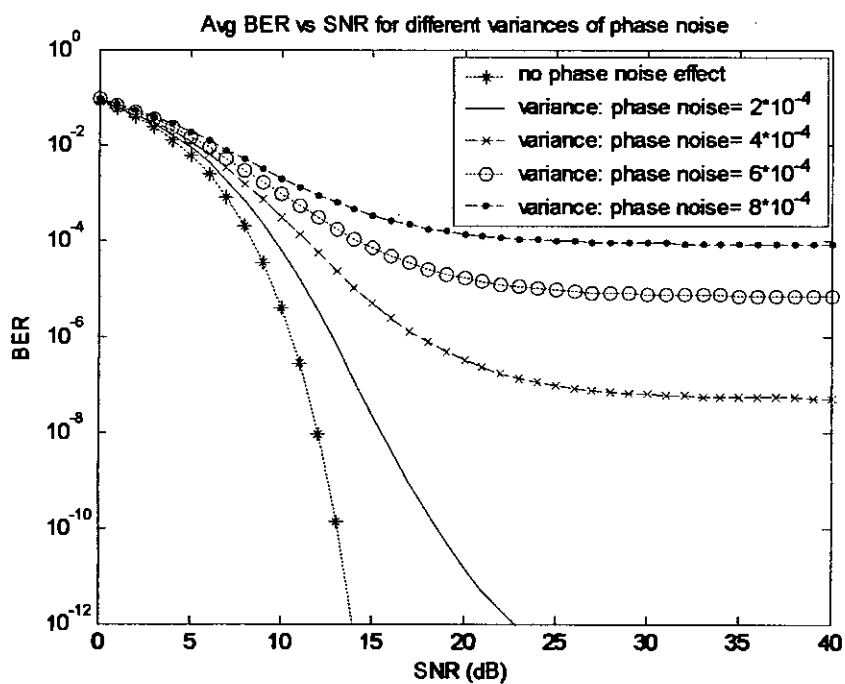

Fig. 5.3: BER performance of a BPSK-OFDM for different variances of phase noise

Fig. 5.4, 5.5 & 5.6 shows the effect of modulation level (M-ary PSK) on the BER performance of an OFDM system considering the effect of CFO, timing jitter and phase noise, respectively. The curves clearly reveal the penalty in SNR as M increases beyond 4. For example in Fig. 5.4, at BER=10^{-5}, the SNR penalty between M=4 and M=8 is approximately 3.5 dB and the difference between M=8 and M=16 is approximately 5dB for a variance of CFO=0.02. However, at M=32 severe performance degradation causes BER floor at 10^{-4} which is unacceptable. Similar curves are shown in Fig 5.4 & 5.6, however, with the increase of modulation level, the performance degradation is the most severe in the case of phase noise.
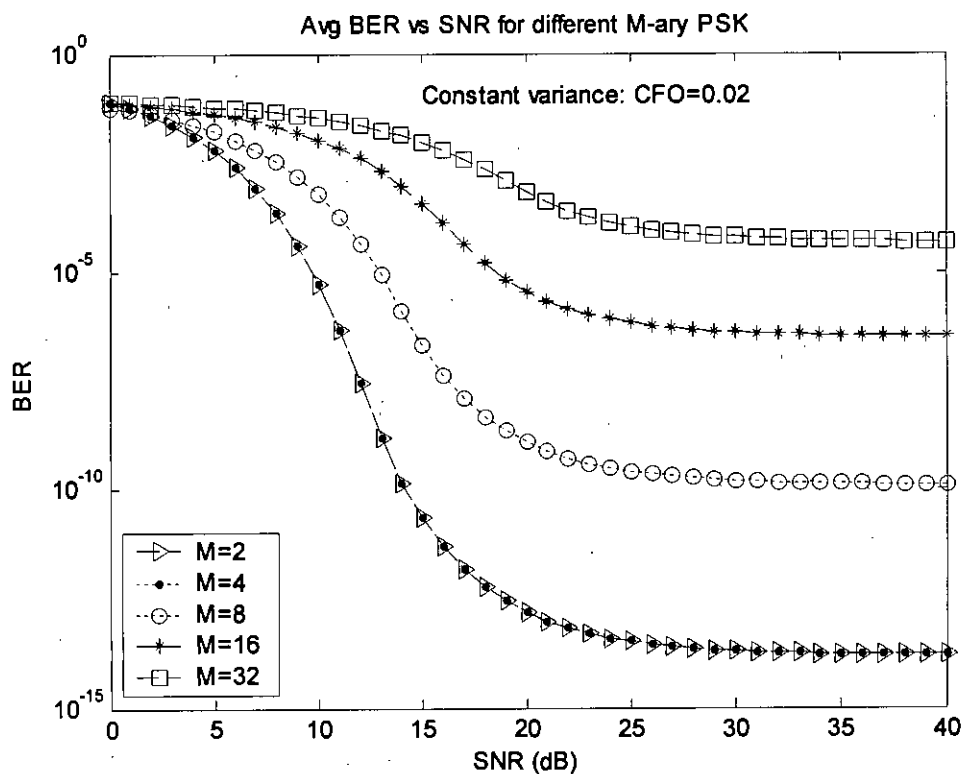

Fig. 5.4: BER performance of M-ary PSK-OFDM for a constant variance of CFO
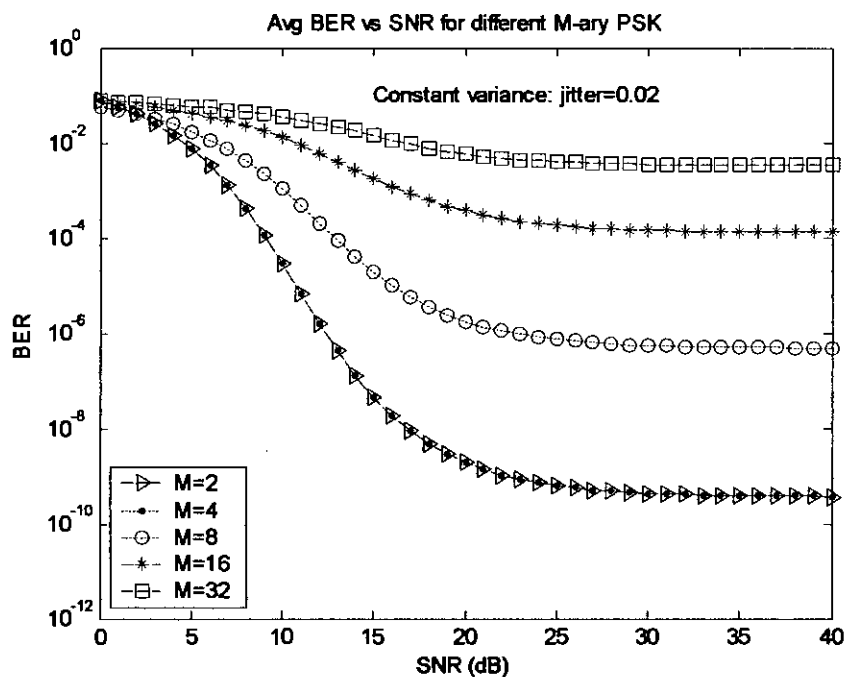
Fig. 5.5: BER performance of M-ary PSK-OFDM for a constant variance of timing jitter
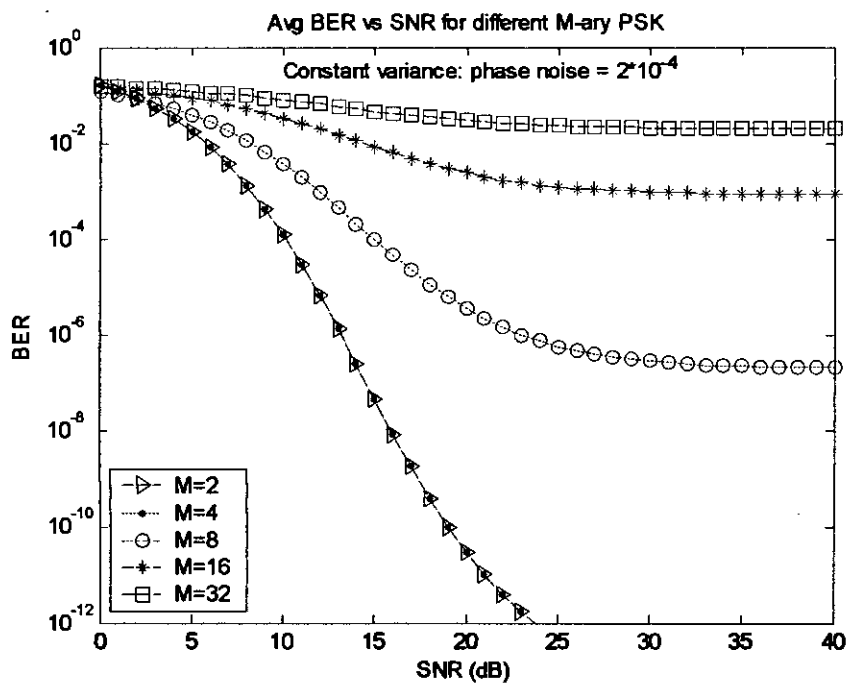

Fig. 5.6: BER performance of M-ary PSK-OFDM for a constant variance of phase noise

Fig. 5.7 shows the BER performance comparisons of CFO, timing jitter and phase noise with their combined effect. It is clear that timing jitter is more sensitive to CFO at a constant variance of 0.02. Phase noise variance is set to a much smaller value of 0.0004 which is 50 times lower than the variances of CFO and jitter, however, the BER performance clearly shows that the system is still more sensitive to phase noise than CFO and jitter.
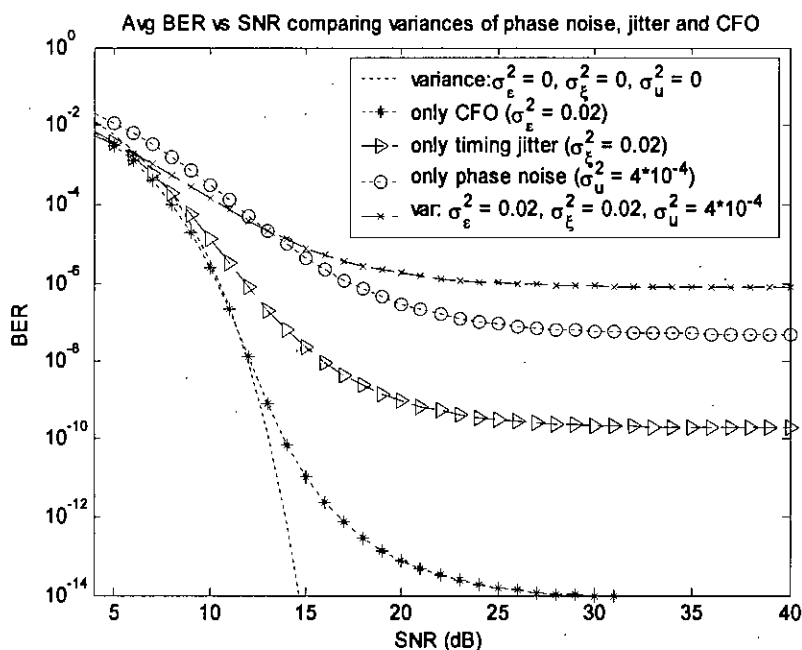
Fig. 5.7: BER performance of an OFDM with individual and combined effects of CFO, timing jitter and phase noise

Fig. 5.8 illustrates the catastrophic effect of CFO, phase noise and timing jitter on the BER performance of an OFDM system. The performance degrades with the increase of the combinational variances of $\sigma_\varepsilon^2, \sigma_u^2$ and σ_ξ^2 , resulting in severe performance degradation which is unacceptable in practice. At high SNRs there exists BER floors resulting from the combined ICI effects, lowering the effective SNRs, and that BER floor runs up when variance level increases. It also implies that OFDM systems with high SNR are more sensitive to ICI, though higher SNR leads to better performance.

The combined influence of CFO, phase noise and jitter on the M-ary PSK-OFDM is depicted in Fig. 5.9. For M>16, severe performance degradation causes very early BER $(BER<10^{-2})$ floors which is unacceptable in practice.
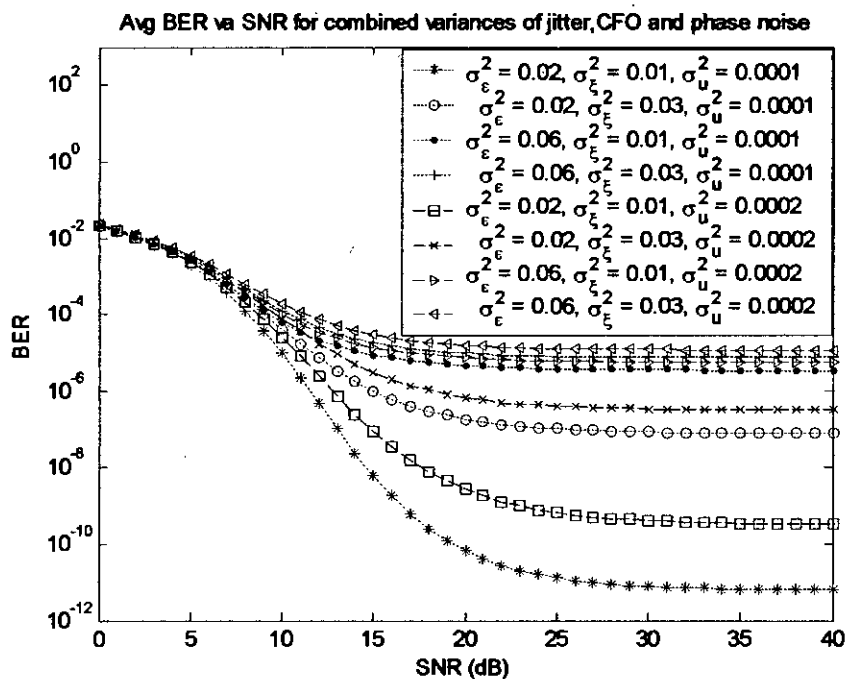
Fig. 5.8: BER performance of a BPSK-OFDM for combined variances of jitter, CFO and phase noise.
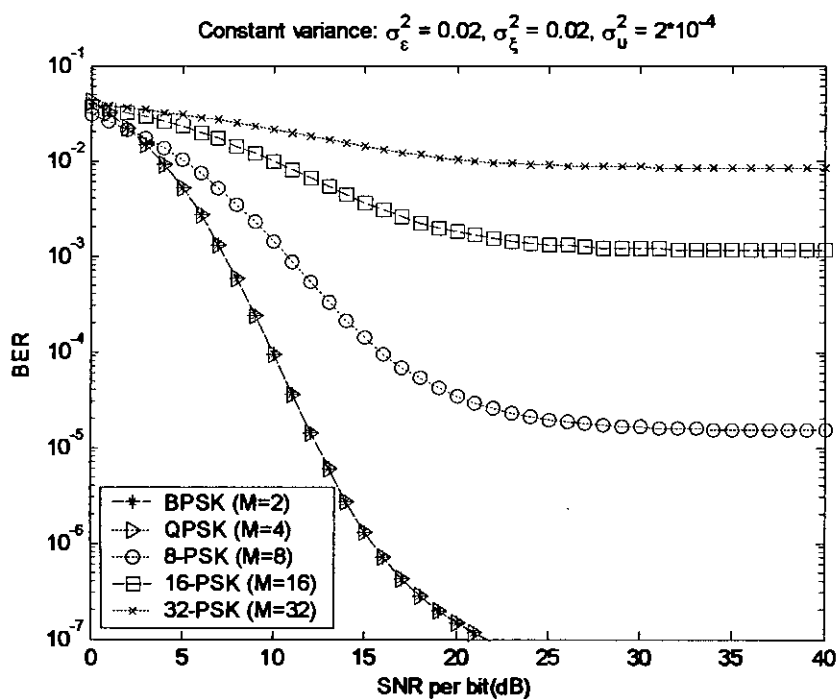
Fig. 5.9: BER performance of M-ary PSK-OFDM for combined variances of jitter, CFO and phase noise.

It is well known that OFDM system performance with imperfect oscillators is strongly dependent on phase noise linewidth, β. As shown in Fig. 5.10, the larger the value of β, the more the SINR penalty is, increasing as a linear function of phase-noise linewidth, β in a logarithmic scale for $\beta > 10^2$ Hz for different values of subcarriers. Hence, the best way to eliminate the detrimental effects of phase noise is to improve oscillator accuracy, and thus decrease phase-noise linewidth. Fig. 5.11 shows the effect of β with the presence of CFO and jitter. As β has no effect on CFO and jitter, similar curves are obtained for the system with approximately a constant 5dB additional penalty resulting from the constant variances of CFO and jitter.
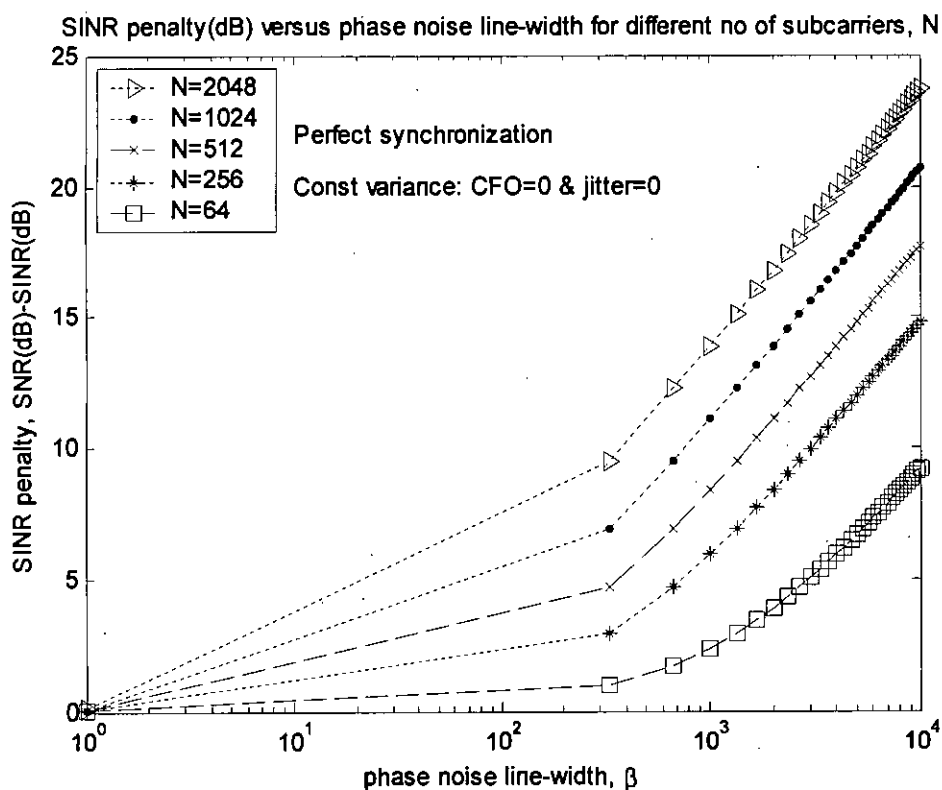
Fig. 5.10: Effect of phase-noise linewidth, β on SINR penalty for different numbers of subcarriers considering perfect synchronization.

SINR penalty(dB) versus phase noise line-width for different no of subcarriers, N
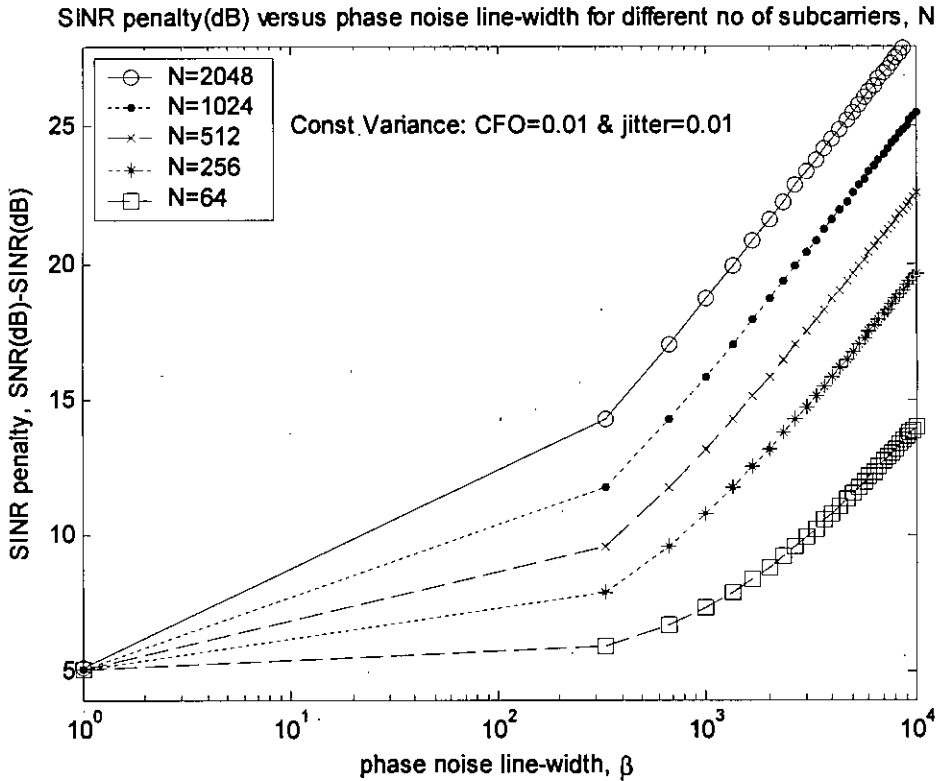
Fig 5.11: Effect of phase-noise linewidth, β on SINR penalty for different numbers of subcarriers considering the presence of CFO and timing jitter.

It is quite straightforward to see that a larger number of subcarriers N lead to worse system performance due to the shorter subcarrier spacing distance, hence, more sensitive to phase noise. In particular, Fig. 5.12 suggests that, when β / R ratio is of the order of 10^{-3} or less, doubling N always causes approximately 3-dB more SINR penalty for all N values. This implies that, when β / R ratio is below a certain level, SINR penalty becomes proportional to the number of subcarriers, N. Fig. 5.13 shows that an approximately 5 dB additional penalty is suffered by the system for all possible values of N in the presence of the constant variances of CFO and jitter. This is because the derived ICI expression (Appendix-I) due to CFO is upper bounded considering $N \approx \infty$.
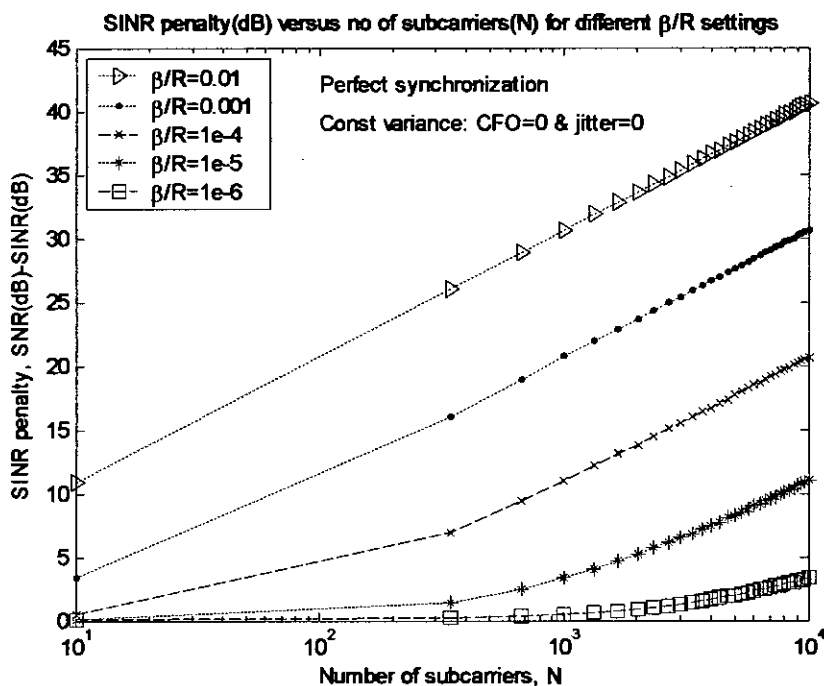
Fig. 5.12: Effect of number of subcarriers, N on SINR penalty for different β / R ratios considering perfect synchronization.
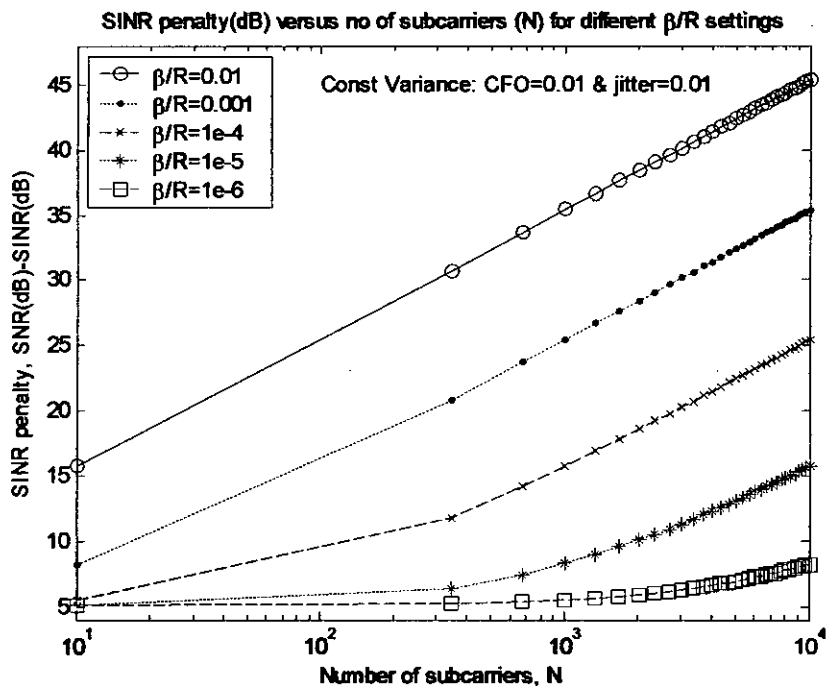
Fig. 5.13: Effect of number of subcarriers, N on SINR penalty for different β / R ratios considering the effect of CFO and timing jitter.

Fig. 5.14 shows that the SINR has a limiting low value for small R/β, regardless of the SNR value which suggests that, for large phase noise (thus, low R/β ratio), a high SNR does not help the performance. Therefore, a well-designed system must have a reasonable ratio in order to achieve adequate performance. In particular, curves show that for very high values of R/β ratio, SINR becomes SNR. This makes sense by noticing that, when R/β goes to infinity, the system is equivalent to a normal one without phase noise. This implies that higher transmission data rate, R results in better system performance. However in Fig. 5.15, SINR never reaches SNR due to a constant penalty suffered by the system under the influence of a constant variance of CFO and jitter.
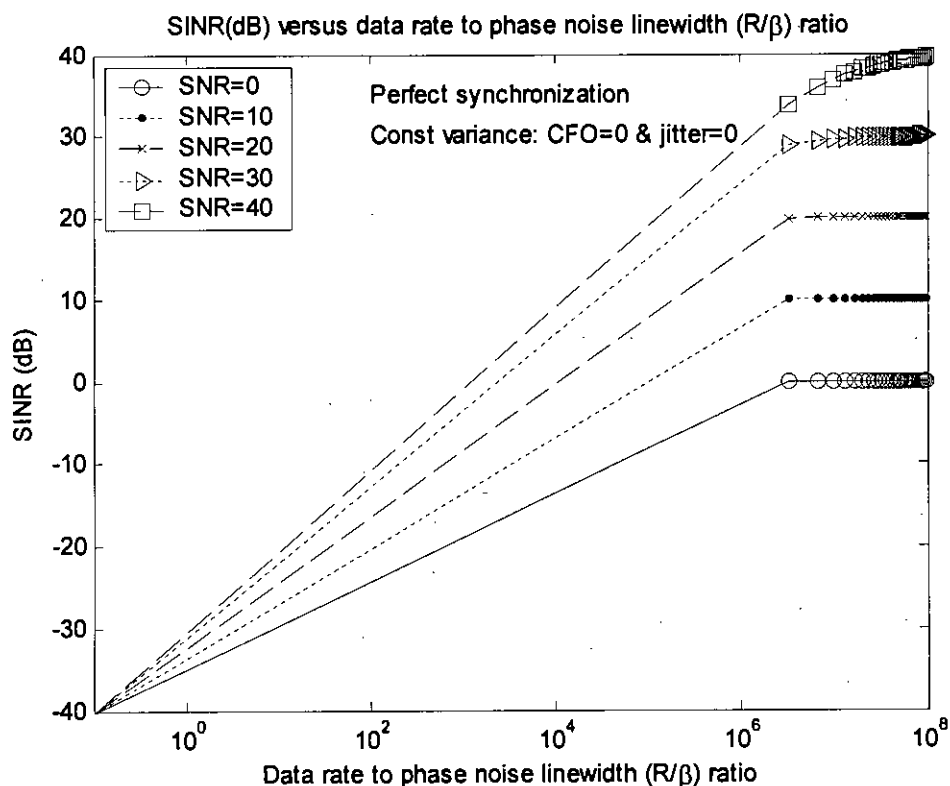
Fig. 5.14: SINR as a function of R/β ratio for different SNR levels considering perfect synchronization.
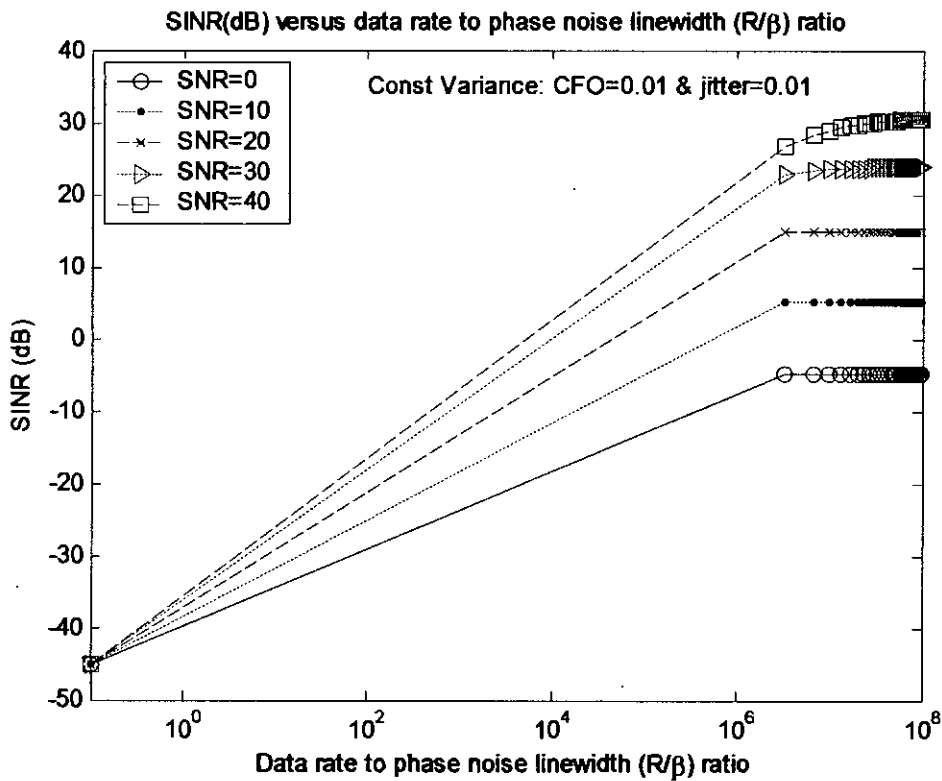
Fig. 5.15: SINR as a function of R/β ratio for different SNR levels considering the effect of CFO and timing jitter.

For low variances of CFO and jitter, SINR is strongly dependent on the values of β and N at higher values of SNR. Here, the sample rate, R is kept constant. As shown in Fig. 5.16, when β is very small compared to the subcarrier spacing, i.e., $\beta N/R$ is of the order of 10^{-4} or less, the ICI due to phase noise is negligible. As a result, there is a constant SINR penalty due to the presence of CFO and timing jitter. Meanwhile, for high phase noise levels with $\beta N/R \geq 1$, SINR penalty exceeds the value of SNR itself, which implying that the ICI overwhelms the desired signals.
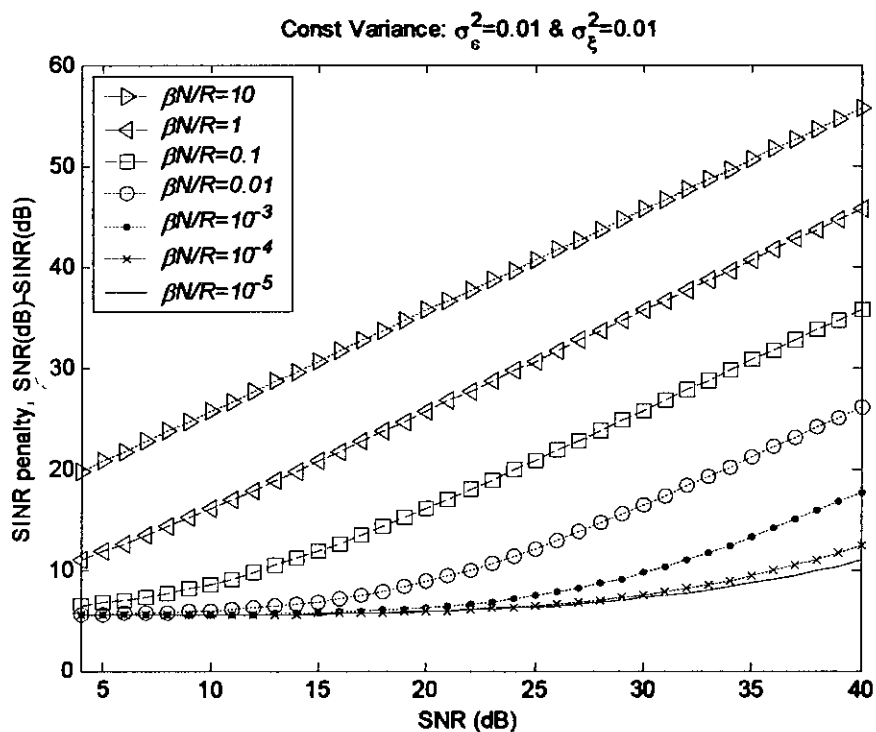
Fig. 5.16: SINR penalty as a function of SNR for different ($\beta N / R$) settings.

Fig. 5.17, 5.18 and 5.19 demonstrates the SINR penalty suffered by the system as a function of $\sigma_\varepsilon^2, \sigma_\xi^2$ and σ_z^2 respectively for a 20dB SNR.

In Fig. 5.17, first of all, we consider the variance of CFO (σ_ε^2) as variable and σ_ξ^2, σ_z^2 as constants. When the variances of jitter and phase noise are zero, ICI occurs only due to CFO. With the increase of σ_ε^2, SINR penalty increases and we can see that nearly 2dB penalty is suffered by the system for $\sigma_\varepsilon^2 = 0.01$. If either or both jitter and phase noise are present along with fading then the system suffers a penalty even at $\sigma_\varepsilon^2 \approx 0$. The SINR penalty curve shifts upwards with the increase of the constant variances of jitter and phase noise.

Similar curves are obtained in Fig. 5.18, for considering σ_ξ^2 as variable and $\sigma_\varepsilon^2, \sigma_z^2$ as constants. From Fig. 5.17 & 5.18, we can see that nearly 1-2dB additional penalty is suffered by the system for jitter than CFO when their respective constant variances have relatively low values.
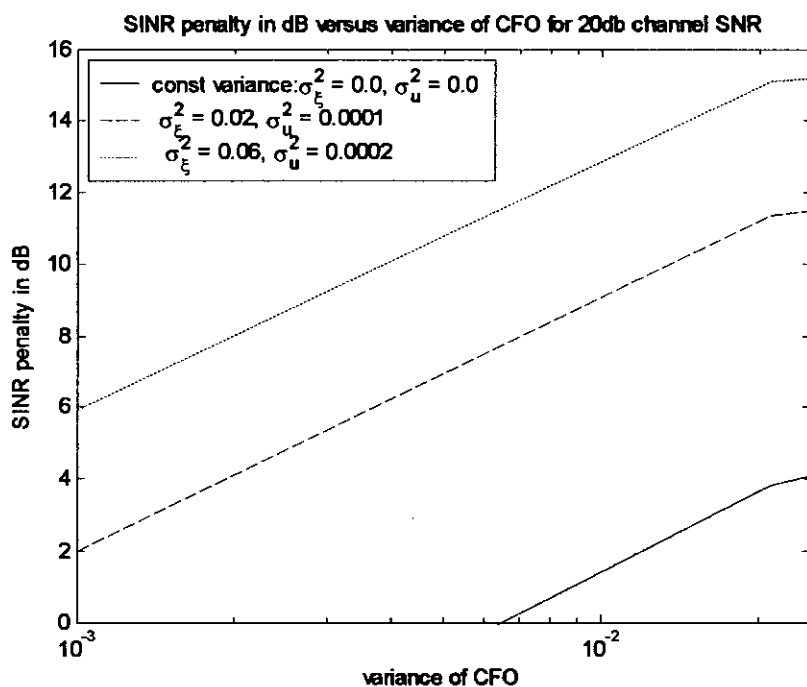
Fig. 5.17: SINR penalty as a function of the variance of CFO for different constant variances of jitter and phase noise.
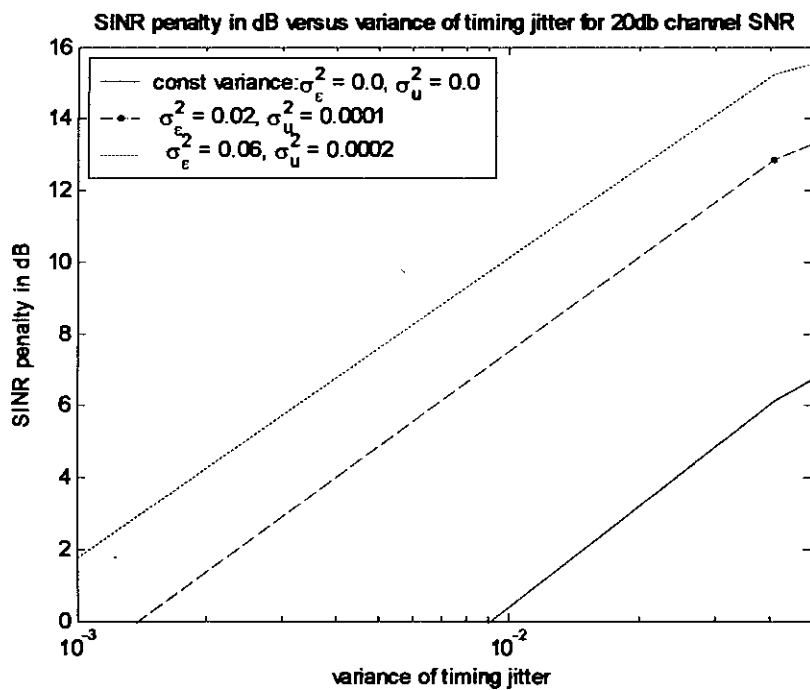
Fig. 5.18: SINR penalty as a function of the variance of timing jitter for different constant variances of CFO and phase noise.

In Fig. 5.19 we see that SINR penalty drastically changes for a very small change in the variances of phase noise. SINR is strongly dependent on the number of sub-carriers (N) as ICI due to phase noise is a function of N . Larger number of N leads to shorter subcarrier spacing distance, hence more sensitive to phase noise and as a result of that SINR penalty increases. It is noticeable that CFO and jitter shows negligible effect on SINR at high values of phase noise variance. From these figures we can conclude that OFDM is more sensitive to phase noise than CFO and jitter.
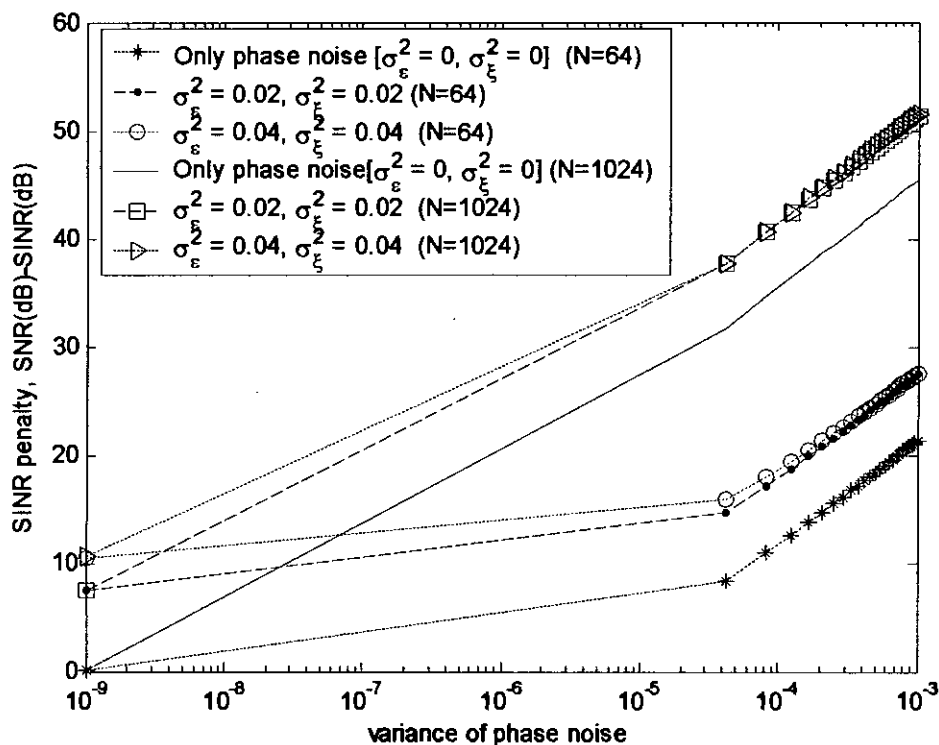
Fig. 5.19: SINR penalty as a function of the variance of phase noise for different constant variances of CFO and jitter with N=64 & N= 1024.

5.3   Performance Results for Turbo-coded OFDM

Fig. 5.20 reflects the comparative BER performance of uncoded and turbo coded BPSK-OFDM system with relatively high variances of all three synchronization impairments. It is known that uncoded OFDM systems with high SNR are more sensitive to ICI. As the coding gain increases for larger ICI effect, the BER performance significantly improves with the increase of SNR level when turbo coding is applied. As shown, a savings of over 10dB is realized in transmitter power (or energy) required to achieve an asymptotic $BER = 10^{-5}$ by applying turbo coding with the parameters listed in Fig. 5.20. It is also possible to achieve a BER as low as 10^{-10} at 10dB SNR through turbo coding for the OFDM systems with synchronization impairments.
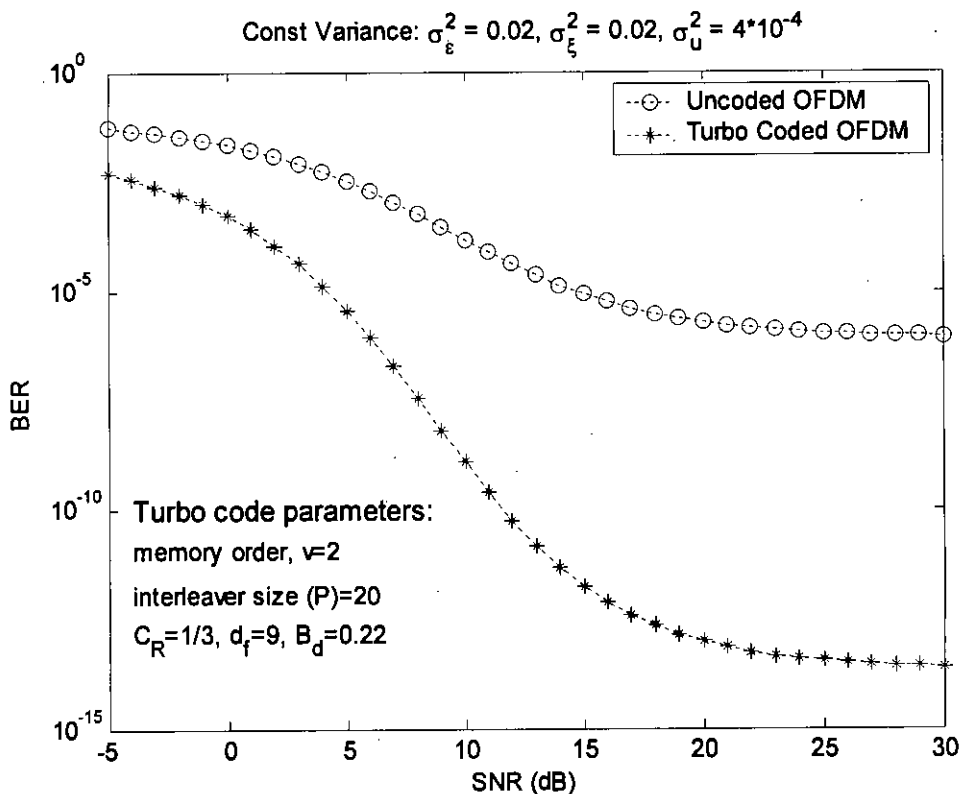
Fig. 5.20: Asymptotic BER performance of turbo coded OFDM system with synchronization impairments

Fig. 5.21 shows the BER performance of a turbo coded OFDM based on distance spectrum (table-3.1) and its average upper bounds (3.4). In the low to medium region of distances, error coefficients for the code with a higher interleaver size are lower. Increasing the interleaver size reduces the error coefficients and thus the effective free distance becomes the dominant parameter even at the lower SNRs. So the code with interleaver size, $P = 50$ has better performance (nearly 2dB coding gain at a BER=10^{-10}) than the code with interleaver size, $P = 20$ in the medium to high SNR region for OFDM systems with synchronization errors.
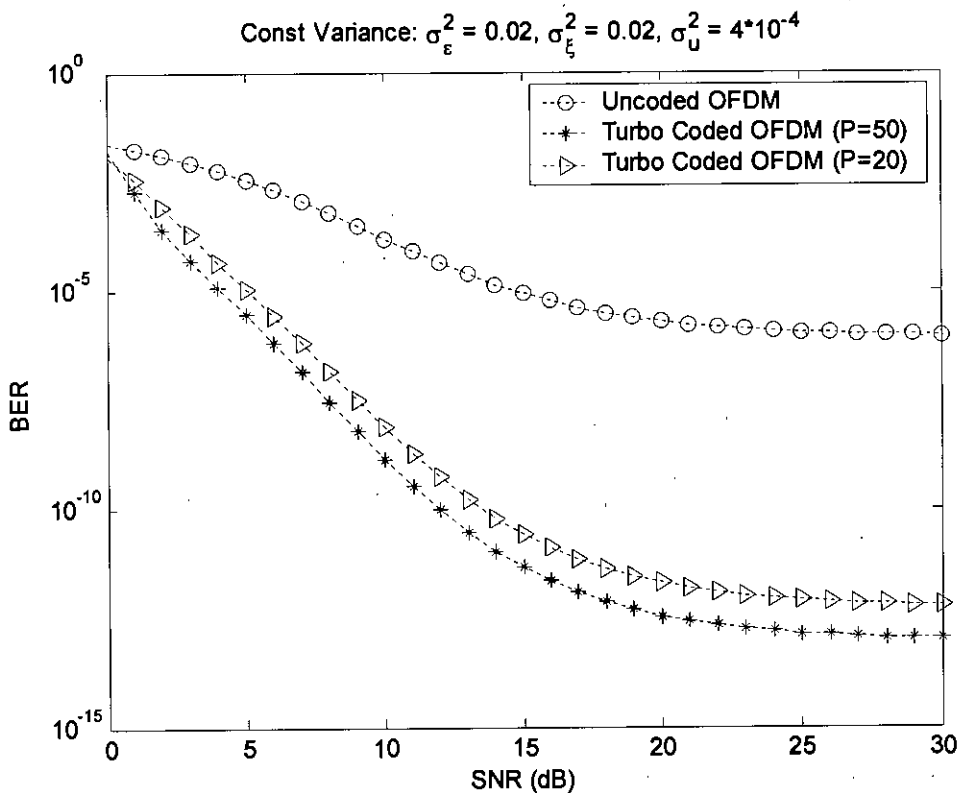
Fig. 5.21: BER upper bounds for turbo coded OFDM system with different interleaver size

Fig. 5.22 reflects the effect of code free distance (d_f) and error coefficients (B_d) respectively on the BER performance of OFDM systems with synchronization impairments. It is clear that BER performance at low SNR's is dominated by the error coefficients. On the other hand at high SNR's, code free distance determines the error performance. For a fixed free distance optimizing the BER probability implies minimization of the error coefficients. So, the code design criteria depend on the region of SNR's where the system is operated. Maximizing the code effective free distance can be used as the design criterion for constructing good turbo codes at high SNR's. However, to design a turbo code at low SNR, it is desirable to have B_d minimized rather than d_f maximized.

Const Variance: $\sigma_\varepsilon^2 = 0.02$, $\sigma_\xi^2 = 0.02$, $\sigma_u^2 = 4*10^{-4}$

Legend:
- $d_f=7, B_d=7.05*10^{-3}$
- $d_f=9, B_d=0.04$
- $d_f=11, B_d=0.12$
- $d_f=13, B_d=0.27$
- $d_f=14, B_d=0.39$

Turbo code parameters:
memory order, $v=2$
interleaver size (P)=20
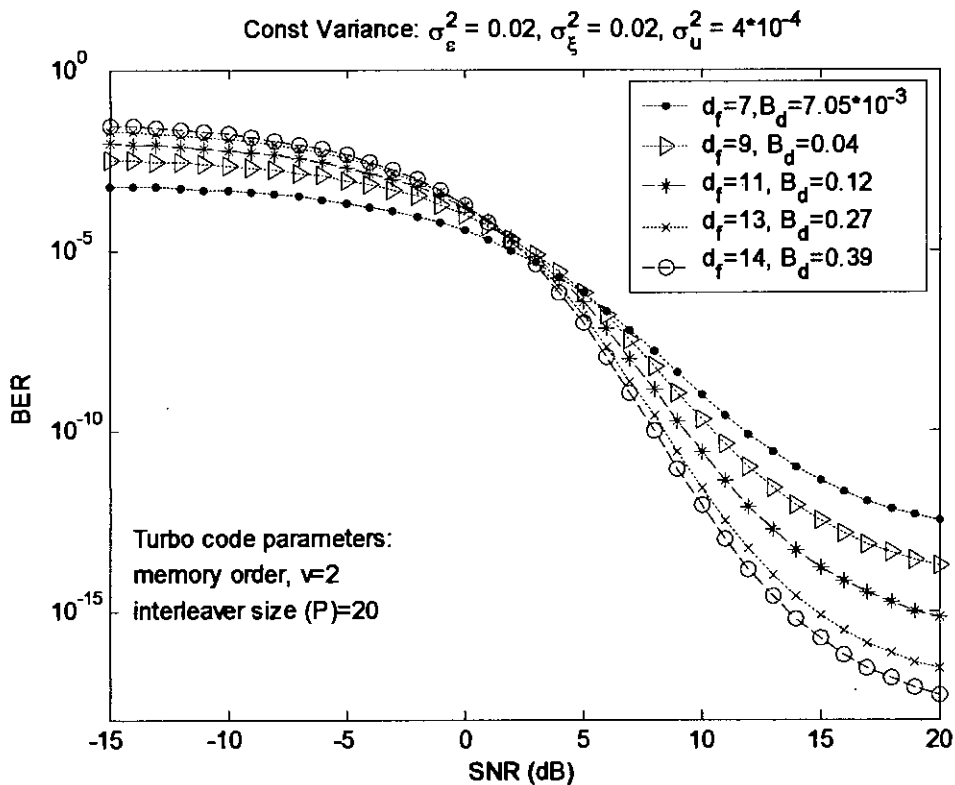
Fig. 5.22: The effect of code distance spectrum on turbo coded OFDM system with synchronization impairments.

5.4   Performance Results for OFDM with Diversity

Fig. 5.23 illustrates the advantage of diversity as a mean for overcoming the severe penalty in SNR caused by fading in multiple paths. Here maximal-ratio-combing (MRC) is used as it gives the best performance improvement as compared with the other methods. At the cost of complicated implementation of 8-receiving antenna it is possible to achieve a BER as low as 10^{-10} at 20dB channel SNR where the system faces severe performance degradation for a single receive antenna (BER<10^{-2}).
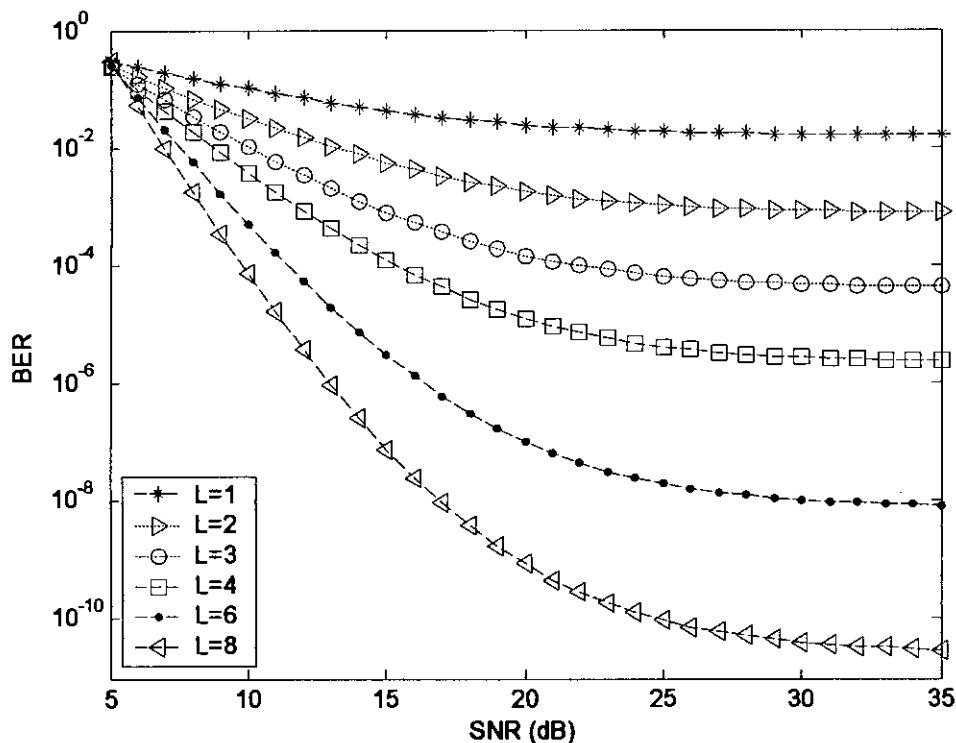
Fig. 5.23: The effect of antenna diversity on the BER performance of an OFDM system under the combined influence of CFO, jitter and phase noise.

5.5 Summary

From the results of numerical analysis, following conclusions may be drawn:

- OFDM is more sensitive to phase noise than CFO or timing jitter. At high SNRs there exist BER floors resulting from the combined ICI effects of CFO, phase noise and jitter, lowering the effective SNRs, and that BER floor runs up when variance level increases. It also implies that OFDM systems with high SNR are more sensitive to ICI, though higher SNR leads to better performance.

- The combined influence of CFO, phase noise and jitter on the M-ary PSK-OFDM clearly reveal the penalty in SNR as M increases beyond 4. For M>16, severe performance degradation causes very early BER floors which is unacceptable in practice.

- When the variances of jitter and phase noise are zero, ICI occurs only due to CFO (σ_ε^2). With the increase of σ_ε^2, penalty increases and nearly 2dB penalty is suffered by the system for $\sigma_\varepsilon^2 = 0.01$. System suffers penalty even at $\sigma_\varepsilon^2 = 0$ if either or both jitter and phase noise are present.

- Nearly 1.5-2 dB additional penalty is suffered by the system for timing jitter than CFO when their respective constant variances have relatively low values.

- SINR penalty drastically changes for a very small change in the variances of phase noise (σ_u^2). It is noticeable that CFO and jitter shows negligible effect on SINR at high values of phase noise variance.

- OFDM system performance with imperfect oscillators is strongly dependent on phase noise linewidth, β. The larger β is, the severe the SINR penalty is, increasing as a logarithmically linear function of phase-noise linewidth, β for $\beta > 10^2$ Hz. Hence, the best way to eliminate the detrimental effects of phase noise is to improve oscillator accuracy, and thus decrease phase-noise linewidth.

- Larger number of subcarriers N lead to worse system performance due to the shorter subcarrier spacing distance, hence, more sensitive to phase noise. When β / R ratio is below a certain level, SINR penalty becomes proportional to the number of subcarriers, N.

- Higher transmission data rate, R results in better system performance. SINR has a limiting low value for small (R / β), regardless of the SNR value which suggests that, for large phase noise (thus, low R / β ratio), a high SNR does not help the performance. Therefore, a well-designed system must have a reasonable R / β ratio in order to achieve adequate performance. In particular, curves show that for very high values of R / β ratio, SINR becomes SNR. However SINR never reaches SNR due to a constant penalty suffered by the system under the influence of a constant variance of CFO and jitter.

- For low variances of CFO and jitter, SINR is strongly dependent on the values of β and N at higher values of SNR for constant data rates. When $\beta \dfrac{N}{R}$ is of the order of 10^{-4} or less, the ICI due to phase noise is negligible. As a result, there is a constant SINR penalty due to the presence of CFO and timing jitter. Meanwhile, for high phase noise levels with $\beta \dfrac{N}{R} \geq 1$, SINR penalty exceeds the value of SNR itself, which implying that the ICI overwhelms the desired signals.

- As the coding gain increases for larger ICI effect, the BER performance significantly improves with the increase of SNR level when turbo coding is applied. A savings of over 10dB is realized in transmitter power (or energy) required to achieve an asymptotic $BER = 10^{-5}$ by applying turbo coding. It is also possible to achieve a BER as low as 10^{-10} at 10dB SNR through turbo coding for the OFDM systems with synchronization impairments.

- Increasing the interleaver size reduces the error coefficients and thus the effective free distance becomes the dominant parameter even at the lower SNRs. So the code with interleaver size, P = 50 has better performance (nearly 2dB coding gain at a BER=10^{-10}) than the code with interleaver size, P = 20 in the medium to high SNR region for OFDM systems with synchronization errors.

- Turbo code design criteria depend on the region of SNR's where the system is operated. Maximizing the code effective free distance can be used as the design criterion for constructing good turbo codes at high SNR's. However, to design a turbo code at low SNR, it is desirable to have the error coefficients minimized rather than code free distance maximized.

- At the cost of complicated implementation of 8-receiving antenna it is possible to achieve a BER as low as 10^{-10} at 20dB channel SNR where the system faces severe performance degradation for a single receive antenna (BER<10^{-2}).

CHAPTER 6

CONCLUSIONS AND FUTURE WORK

The thesis has mainly dealt with the combined influence of carrier frequency offset (CFO), phase noise and timing jitter on the performance of OFDM systems. The essential contributions and summary of the thesis are discussed below

- OFDM is very much sensitive to the synchronization errors, for example, CFO, timing jitter and phase noise. These synchronization impairments cause ICI and severe BER performance degradation. Channel coding and interleaving along with diversity reception can improve the performance of OFDM with synchronization impairments over frequency selective fading channels.

- The derivation of an exact closed form expression for the Signal-to-Interference-plus-Noise Ratio (SINR) under the combined influence of CFO, phase noise and timing jitter is one of the most important contributions in this work [30]-[31]. The combined effects of CFO, phase noise and timing jitter are exhibited by expressing the OFDM system BER performance as a function of its critical parameters. The SINR and BER expression for the system shows that in the presence of all three synchronization impairments, several parameters affect OFDM system performance, resulting in severe performance degradation which is unacceptable in practice.

- Results show that OFDM is more sensitive to phase noise than CFO and timing jitter and the performance degradation also depends on several critical parameters, such as number of subcarriers, phase noise linewidth, transmission data rate and SNR.

- Significant performance improvement is achieved through turbo coding and antenna diversity reception for OFDM systems with synchronization impairments.

Some challenges remain for future work:

o The estimation techniques and the compensation schemes of the combined influence of CFO, phase noise and timing jitter for OFDM systems may be developed in the future.

o The research can be extended to STBC-OFDM and multiuser OFDM (OFDMA) systems.

o High peak to average power ratio (PAPR) is a major drawback in OFDM systems due to the non-linear behavior of power amplifiers (PA). The resulting clipping effects give rise to ICI and severe performance degradation. This effect can be modeled along with the synchronization impairments.

REFERENCES

[1]   "Wireless LAN Medium Access Control (MAC) and Physical Layer (PHY) Specifications: High-speed Physical Layer in the 5 GHz Band," *IEEE Std.* 802.11a, 1999.

[2]   "Wireless LAN Medium Access Control (MAC) and Physical Layer (PHY) Specifications. Amendment 4: Further Higher Data Rate Extension in the 2.4 GHz Band," *IEEE Std.* 802.11g, 2003.

[3]   Steendam, H. and Moeneclaey, M., "Synchronization Sensitivity of Multicarrier Systems," *Euro. Trans. Telecomms.,* vol. 15, pp. 223-234, 2004.

[4]   Moose, P.H., "A Technique for Orthogonal Frequency-Division Multiplexing Frequency Offset Correction," *IEEE Trans. Commun.,* vol. 42, pp. 2908-2914, Oct. 1994.

[5]   Wu, S. and Bar-Ness, Y., "OFDM Systems in the Presence of Phase Noise: Consequences and Solutions," *IEEE Trans. Commun.,* vol. 52, No. 11, pp. 1988-1996, Nov. 2004.

[6]   Tomba, L. and Krzymien, W.A., "A Model for the Analysis of Timing Jitter in OFDM Systems," in *Proc. IEEE Int. Conf. Commun. (ICC 98),* vol. 3, pp. 1227-1231, June 1998.

[7]   Armstrong, J., "Analysis of New and Existing Methods of Reducing Intercarrier Interference Due to Carrier Frequency Offset in OFDM," *IEEE Trans. Commun.,* vol. 47, pp. 365-369, March 1999.

[8]   Pollet, T., Bladel M. van and Moeneclaey, M., "BER Sensitivity of OFDM Systems to Carrier Frequency Offset and Wiener Phase Noise," *IEEE Trans. Commun.,* vol. 43, pp. 191-193, Feb. 1995.

[9]   Huang, D.D. and Letaief, K.B., "Carrier Frequency Offset Estimation for OFDM Systems Using Null Subcarriers," *IEEE Trans. Commun.,* vol. 54, no. 5, pp. 813-823, May 2006.

[10]   Armada, A.G., "Understanding the Effects of Phase Noise in Orthogonal Frequency-Division Multiplexing (OFDM)," *IEEE Trans. Broadcast.,* vol. 47, pp. 153-159, June 2001.

[11]   Tomba, L., "On the Effect of Wiener Phase Noise in OFDM System," *IEEE Trans. Commun.,* vol. 46, pp. 580-583, May 1998.

[12]   Zhang, Y. and Liu, H., "MIMO-OFDM Systems in the Presence of Phase Noise and Doubly Selective Fading," *IEEE Trans. Veh. Technol.,* vol. 56, no. 4, pp. 2277-2285, July 2007.

[13]   Zogakis, T.N. and Cioffi, J.M., "The effect of timing jitter on the performance of a discrete multitone system," *IEEE Trans. Commun.,* vol. 44, no. 7, pp. 799-808, July 1996.

[14]   Pollet, T. and Moeneclaey, M., "Synchronizability of OFDM signals," in *Proc. Globecom'95,* pp. 2054-2058, Singapore, Nov. 1995.

[15]   Springer, A. and Weigel, R., *UMTS The Universal Mobile Telecommunications Systems.* Springer-Verlag, 2002.

[16]   Proakis, J.G., *Digital Communications,* 4th ed. New-York, Mcgraw-Hill Book Company, 2001.

[17]   Molisch, A.F., *Wireless Communications.* John Wiley & Sons Ltd., 2005.

[18]   Rappaport, T.S., *Wireless Communications Principles & Practice.* Prentice Hall, Inc., 1996.

[19]   Hanzo, L., Münster, M., Choi, B.J. and Keller, T., *OFDM and MC-CDMA.* West Sussex, Piscataway, NJ, England: Wiley, IEEE Press, 2003.

[20]   Chang, R.W., "Synthesis of Band-limited Orthogonal Signals for Multichannel Data Transmission," in *The Bell System Technical Journal,* vol. 45, pp. 1775-1976, Dec. 1966.

[21]   Weinstein, S.B. and Ebert, P.M., "Data Transmission by Frequency-Division Multiplexing Using the Discrete Fourier Transform," in *IEEE Communications Magazine,* vol. 19, No. 5, pp. 628-634, Oct. 1971.

[22]   Bahai, Ahmad R.S., Singh, M., Goldsmith, A. J. and Saltzberg, B. R., "A New Approach for Evaluating Clipping Distortion in Multicarrier Systems," *IEEE Trans. on Selected Areas in Commun.,* vol. 44, no. 7, pp. 799-808, July 1996.

[23]   Stott, J.H., "The How and Why of COFDM," in *EBU technical Review,* Winter 1998.

[24]   Berrou, C., Glavieux, A. and Thitimajshima, P., "Near Shannon Limit Error-Correcting Coding and Decoding: Turbo-Codes", in *Proc. of ICC'93,* Geneve, pp. 1064–1070, May 1993.

[25]   Vucetic, B. and Yuan, J., *Turbo Codes: Principles and Applications,* Kluwer Academic Publishers, 2000.

[26] Benedetto, S. and Montorsi, G., "Design of parallel concatenated convolutional codes," *IEEE Trans. Commun.*, vol. 44, No. 5, pp. 591-600, May 1996.

[27] Yuan, J., Vucetic, B. and Feng, W., "Combined turbo codes and interleaver design," *IEEE Trans. Commun.*, vol. 47, no. 4, pp. 484-487, April 1999.

[28] Murch, Ross D. and Letaief, K.B., "Antenna Systems for Broadband Wireless Access" *IEEE Communications Magazine*, April 2002.

[29] Burr, A.G., "Multilevel Modulation and Coding for Indoor Radio Channels," *IEE Colloquium on Radio LANs and MANs*, pp. 7/1-7/5, April 1995.

[30] Mallick, Shankhanaad, Ahmed, I. and Majumder, S.P., "Analytical Performance Evaluation of an OFDM System in the Presence of Carrier Frequency Offset, Phase Noise and Timing Jitter," accepted for publication *in the Proceedings of IEEE, TENCON*, 2008.

[31] Mallick, Shankhanaad and Majumder, S.P., "Performance Analysis of an OFDM System in the Presence of Carrier Frequency Offset, Phase Noise and Timing Jitter over Rayleigh Fading Channels," accepted for publication *in the Proceedings of ICECE*, 2008.

APPENDIX-I

$$E[|I_1(k)|^2] = |X|^2|H|^2(\sin \pi\varepsilon)^2 \sum_{\substack{r=0 \\ r\neq k}}^{N-1} \frac{1}{\{N\sin\frac{\pi(r-k+\varepsilon)}{N}\}^2} \qquad (A.1)$$

Let, $r - k = p$.

When, $r = 0$, $p = -k$;

When, $r = N-1$, $p = N-1-k$;

$$\text{So, } E[|I_1(k)|^2] = |X|^2|H|^2(\sin \pi\varepsilon)^2 \sum_{\substack{p=-k \\ p\neq 0}}^{N-1-k} \frac{1}{\{N\sin\frac{\pi(p+\varepsilon)}{N}\}^2} \qquad (A.2)$$

The sum in (A.2) can be bounded for $\varepsilon = 0$. It consists of N positive terms. The interval of the sum is contained within the interval $0 \le p \le N-1$ and its location is dependent on k. Also note the following; the argument of the sum is periodic with period N, it is an even function of p, and it is even about $p = N/2$. Thus the N terms of the sum can be divided in the intervals $-N/2 \le p \le -1$ and $1 \le p \le N/2$ for every k. Consequently,

$$\sum_{\substack{p=-k \\ p\neq 0}}^{N-1-k} 1/\{N\sin(\pi p/N)\}^2 < 2\sum_{p=1}^{N/2} 1/\{N\sin(\pi p/N)\}^2 \qquad (A.3)$$

Observe that $\{\sin(\pi p/N)\}^2 \ge (2p/N)^2$ for $|p| \le N/2$. Therefore,

$$2\sum_{p=1}^{N/2} 1/\{N\sin(\pi p/N)\}^2 < 2\sum_{p=1}^{N/2} 1/(2p)^2 < \frac{1}{2}\sum_{p=1}^{N/2} 1/p^2 < \frac{1}{2}\sum_{p=1}^{\infty} 1/p^2 = \frac{\pi^2}{12} = 0.82 \qquad (A.4)$$

Upper bounds the sum in (A.2) for very small ε. In [4] the sum in (A.2) has been evaluated numerically to be bounded by 0.5947 for $|\varepsilon| \le 0.5$ so that

$$E[|I_1(k)|^2] \le 0.5947|X|^2|H|^2(\sin \pi\varepsilon)^2; \qquad |\varepsilon| \le 0.5 \qquad (A.5)$$

APPENDIX-II

Energy of $\Theta(r)$

The DFT response of $\varphi_m(n)$ is given by

$$\Theta(r) = \frac{1}{N}\sum_{n=0}^{N-1}\varphi(n)e^{-j\frac{2\pi}{N}nr}$$

$$= \frac{1}{N}\sum_{n=0}^{N-1}[C_m + \sum_{i=0}^{n}u(T_m+i)]e^{-j\frac{2\pi}{N}nr}$$

$$= C_m[\frac{1}{N}\sum_{n=0}^{N-1}e^{-j\frac{2\pi}{N}nr}] + \frac{1}{N}\sum_{n=0}^{N-1}\sum_{i=0}^{n}u(T_m+i)e^{-j\frac{2\pi}{N}nr}$$

$$= \frac{1}{N}\sum_{n=0}^{N-1}\sum_{i=0}^{n}u(T_m+i)e^{-j\frac{2\pi}{N}nr}; \quad [\because \frac{1}{N}\sum_{n=0}^{N-1}e^{-j\frac{2\pi}{N}nr} = 0 \; for \; r=1,2,...,N-1]$$

$$= \frac{1}{N}\sum_{n=0}^{N-1}u(T_m+n)\sum_{i=n}^{N-1}e^{-j\frac{2\pi}{N}ir}$$

$$= \frac{1}{N}\sum_{n=0}^{N-1}u(T_m+n)\cdot\frac{e^{-j\frac{2\pi}{N}nr}-1}{1-e^{-j\frac{2\pi}{N}r}}$$

$$= \frac{-1}{N\sin(\frac{\pi r}{N})\cdot e^{-j\frac{\pi}{N}r}}\sum_{n=0}^{N-1}u(T_m+n)\cdot\sin(\frac{\pi rn}{N})e^{-j\frac{\pi}{N}rn}$$

Hence according to the mutual independence of Gaussian random variables $u(i)$'s, we can calculate the energy of $\Theta(r)$ as

$$E[|\Theta(r)|^2] = \frac{\sigma_u^2}{N^2\sin^2(\frac{\pi r}{N})}\sum_{n=0}^{N-1}\sin^2(\frac{\pi rn}{N})$$

$$= \frac{\sigma_u^2}{2N\sin^2(\frac{\pi r}{N})}$$

Since for $r \neq 0$ and for even N, $\sum_{n=0}^{N-1}\sin^2(\frac{\pi rn}{N}) = \frac{N}{2}$